12-2021

Digital design and thermomechanical process simulation for 3D printing with ABS and soyhull fibers reinforced ABS composites.

Saleh Khanjar
University of Louisville

DIGITAL DESIGN AND THERMOMECHANICAL PROCESS SIMULATION
FOR 3D PRINTING WITH ABS AND SOYHULL FIBERS REINFORCED ABS
COMPOSITES

By
Saleh Khanjar
B.S Mechanical, University of Gaziantep, 2019

A Thesis
Submitted to the faculty of the

J.B. Speed School of Engineering of University of Louisville

In Partial Fulfillment of the Requirements
For the Degree of

Master of Science
in Mechanical Engineering

Department of Mechanical
EngineeringUniversity of
Louisville
Louisville, Kentucky

December 2021

DIGITAL DESIGN AND THERMOMECHANICAL PROCESS SIMULATION
FOR 3D PRINTING WITH ABS AND SOYHULL FIBERS REINFORCED ABS
COMPOSITES

By
Saleh Khanjar
B.E Mechanical, University of Gaziantep, 2019

A Thesis Approved on

November 30, 2021

by the following Thesis Committee:

<div style="text-align:center">

Dr. Kunal Kate

Dr. Sundar Atre

Dr. Jagannadh Satyavolu

</div>

DEDICATION

This work would not have been possible without the financial support from USB, VENOSA and MBDA (Minority Business Development Agency).

I would like to express my deep sense of gratitude and profound respect towards my advisor Dr. Kunal Kate of J.B. Speed School of Engineering at University of Louisville, who has helped and encouraged me at all stages of my thesis work with great patience. Throughout the course of my research journey, he has directed me in the right direction and given me great support throughout the work process. Without his guidance and persistent help this thesis would not have been possible.

I would also like to thank Dr. Sundar Atre for giving me the opportunity to join his research group, Materials Innovation Guild and AMIST. Throughout my research journey, he always encouraged me to express my ideas. He guided me through tough times and was with me to check on my research progress. His sincere dedication to his students is both admirable and inspirational. It was a privilege to work with him and learn from him.

Thanks to Dr. Jagannadh, Dr. Roshan and Dr. Osama for their personal support in preparing this thesis and sharing their expertise and knowledge with me during my work with their research group.

A special thanks to my colleagues Param, Qasim, Kavish, Arul, Pavan, Athira and Amber. without their help and support I would not be able to go through

all the challenges.

Finally, I would like to thank everyone who helped me and encouraged me directly or indirectly.

ABSTRACT

DIGITAL DESIGN AND THERMOMECHANICAL PROCESS SIMULATION
FOR 3D PRINTING WITH ABS AND SOYHULL FIBERS REINFORCED ABS
COMPOSITES

Saleh Khanjar

November 30, 2021

Recent demonstrations with fused filament fabrication (FFF) 3D printing have shown
to produce prototypes as well as production components. Additionally, due to the FFF
process platforms being low-cost and readily available there has been a high-demand to
produce on-demand parts for various applications in automotive, in-space manufacturing
and electronic industries. However, current limitations such as limited availability of
advanced composites materials, and guidelines for design-for-manufacturing make the
process prone to trial-and-error experiments both at the materials development, product
design and manufacturing stage. In this work, new thermomechanical process simulations
platform, Digimat-AM has been evaluated to address and demonstrate digital design and
manufacturing of FFF process by performing simulation and experiments. With the use of
Acrylonitrile butadiene (ABS) material and soyhull fibers reinforced ABS composite
(ABS-SFRC) as a basis, an L9 Taguchi design-of-experiment (DOE) was setup by varying
key process input parameters for FFF 3D printing such as layer thickness, melt temperature
and extrusion multiplier were varied for three levels. A total of 9 DOE simulations and

experiments were performed to compare part properties such as dimensions, warpage, and print time were analysed. Additionally, ANOVA analysis was performed to identify the optimum and the worst conditions for printing and correlate them with their effect on the mechanical properties of the printed samples. Furthermore, from the simulation results, a reverse warpage geometry, 3D model was generated that factors for part warpage, shrinkage, or other defects to enable 3D printing parts to design dimensions. Subsequently, using the generated reversed warpage geometry was used to perform 3D printed experiments and analyzed for part dimensions and defects. As a case study, a functional prototype [Two different geometries] was designed and simulated on Digimat-AM and using the above guide, 3D printing was performed to obtain part to specific dimensions.

In addition to that, the thermomechanical properties of ABS-SFRC were needed to perform the Digimat simulation of geometries printed with ABS-SFRC. However, the materials property database of ABS-SFRC is very limited and experimental measurements can be expensive and time consuming. This work investigates models that can predict soyhull fibers reinforced polymer material composite properties that are required as input parameters for simulation using the Digimat process design platform for fused filament fabrication. ABS-SFRC filaments were made from 90% ABS 10% soyhull fibers feedstock using pilot scale filament extrusion system. Density, specific heat, thermal conductivity, and Young's modulus were calculated using models. The modeled material properties were used to conduct simulations to understand material-processing-geometry interactions.

TABLE OF CONTENTS

LIST OF TABLES

LIST OF FIGURES

LIST OF EQUATIONS

CHAPTER 1

INTRODUCTION

Fused filament fabrication, also known as fused deposition modeling, or called filament freeform fabrication, is a 3D printing process that uses a continuous filament of a thermoplastic material. The filament is fed from a large spool through a moving, heated printer extruder head, and is deposited on the growing work. Filament's materials are mainly thermosets or thermoplastic materials like (ABS, Nylon, PLA, TPU..etc..). more advanced material composites with carbon fibers or glass fibers have shown enhanced mechanical properties. But the higher cost of carbon fibers and glass fibers is one of the drawbacks compared to natural fibers like the fibers extracted from soybean hulls.

The development of a variety of new material classes for FFF has been a focus for both the research and industrial communities for a while. As a result, new classes of materials such as composite materials with polymeric matrix and short or long hard fibers, ceramic, food pastes and biological pastes have been successfully printed by FFF. However, currently, limited guidelines for design-for-manufacturing make the process prone to trial-and-error experiments not only at the materials development stage but also at the product design and manufacturing stage.

In FFF, as the extrudate from the nozzle is deposited on the substrate, being at high temperature it dissipates heat to the environment through convection and radiation. As it cools down, conduction within the printed material and with the build plate leads to heat transfer to the deposited layer. While the deposited semi-molten material is in the transition phase of solidification, new incoming layers on top of it are at a higher temperature and transfer heat to the previously deposited layer thereby increasing its temperature. The multiple cooling and heating cycles lead to non-uniform volumetric changes in the deposited material. Moreover, a thermal gradient gets developed along Z-axis. These phenomena induce residual stresses in the printed component in an anisotropic manner. These stresses consequently produce part distortions and nonuniform variations in dimensions, during the printing process as well as during cooling after printing and component removal from the build plate. This phenomenon depends not only on processing conditions but also on material properties and part geometry. Hence, material properties, part design and process parameters have a significant influence on printed part quality. Part distortions and dimensional variations are the most significant quality challenges that hinder acceptance of the FFF process and printed parts in potential functional applications. Hence, the influence of each variable on part quality needs to be investigated. Prediction of the thermal gradient, residual stresses and distortion will enable minimizing the trial-and-error experimental approach in research and also facilitate design for FFF.

In CHAPTER 2 Thermomechanical simulation studies have been conducted. In this study, the applicability of the finite element analysis simulation for the FFF printing process was investigated. A commercial software (Digimat 2019.0 from MSC Software) was used to simulate the printing process. A thermo-mechanical material model was

considered for the filament material. Printed part quality was evaluated in terms of part distortion and change in dimensions. Simulation results were verified with experimental printing and measurements. The predictive simulation tool allows assessment of the printing process outcomes at the part design stage based on the part geometry, material properties, print strategy and process conditions enabling design for additive manufacturing (DfAM). For a given material, the identification of optimal processing conditions and part design enables getting the part right and printed right first time as opposed to the traditional approach based on experience and trial-and-error method.

In CHAPTER 3 the thermomechanical properties of soyhull fiber reinforced ABS composite or ABS-SFRC as we will be referring to it in this study, have been calculated using the standard thermomechanical properties of pure ABS polymer and estimates of the thermomechanical properties of soyhull fibers based on previous studies and literature of natural fiber thermomechanical properties. Like Chapter 2 a thermomechanical simulation using Digimat 2021 was conducted to determine warpages in geometry printed with the ABS-SFR filament. ABS-SFR filament were prepared using pilot scale filament extrusion process. Best and worst warpage process conditions were experimentally verified by 3D printing the geometry and comparing actual warpages with simulated warpages. Finally, comparison between warpage results of pure ABS from chapter 2 and ABS-SFR warpage results has been compared to evaluate material properties effects on the warpage results.

CHAPTER 2

DIGITAL DESIGN AND MANUFACTURING WITH THERMOMECHANICAL

PROCESS SIMULATION FOR FUSED FILAMENT FABRICATION 3D PRINTING [1]

2.1 INTRODUCTION

Fused filament fabrication (FFF) is one of the most widely used additive manufacturing (AM) processes because it uses inexpensive equipment and it can print most of the widely used polymeric materials. In FFF, a thermoplastic material is heated to a semi-molten state, extruded through a nozzle as a thin filament. The heated extrusion head moves in a toolpath predefined by part geometry, thereby depositing extrudate on top of a build plate or an existing layer to build a three-dimensional part layer-by-layer. Being efficiently implemented at both desktop and industrial level printing, FFF finds the widest demand to produce on-demand parts for various applications across industries ranging from automotive to biomedical, in-space manufacturing and electronic industries [1].

The development of a variety of new material classes for FFF has been a focus for both the research and industrial communities for a while. As a result, new classes of materials such as composite materials with polymeric matrix and short or long hard fibers, ceramic, food pastes and biological pastes have been successfully printed by FFF [2].

4

However, currently, limited guidelines for design-for-manufacturing make the process prone to trial-and-error experiments not only at the materials development stage but also at the product design and manufacturing stage.

In FFF, as the extrudate from the nozzle is deposited on the substrate, being at high temperature it dissipates heat to the environment through convection and radiation. As it cools down, conduction within the printed material and with the build plate leads to heat transfer to the deposited layer [4]. While the deposited semi-molten material is in the transition phase of solidification, new incoming layers on top of it are at a higher temperature and transfer heat to the previously deposited layer thereby increasing its temperature. The multiple cooling and heating cycles lead to non-uniform volumetric changes in the deposited material. Moreover, a thermal gradient gets developed along Z-axis. These phenomena induce residual stresses in the printed component in an anisotropic manner. These stresses consequently produce part distortions and nonuniform variations in dimensions, during the printing process as well as during cooling after printing and component removal from the build plate. This phenomenon depends not only on processing conditions but also on material properties and part geometry [4] [5]. Hence, material properties, part design and process parameters have a significant influence on printed part quality. Part distortions and dimensional variations are the most significant quality challenges that hinder acceptance of the FFF process and printed parts in potential functional applications [3]. Hence, the influence of each variable on part quality needs to be investigated. Prediction of the thermal gradient, residual stresses and distortion will enable minimizing the trial-and-error experimental approach in research and also facilitate design for FFF.

The role of part geometry in additive manufacturing is a frequently studied subject. Pennington et al. [6] investigated factors that affect dimensional accuracy in FFF through an experimental study. Part geometry and extrusion temperature were reported of having a significant effect. Jiang and Gu [7] studied rheology phenomena in FDM and recommended critical process parameters with consideration to the final part's dimensional accuracy.

However, in this context, computational simulations aiming at predicting residual stresses and part deformation are attracting more and more interest in additive manufacturing as an alternative to experiments to study the effect of process parameters on the 3D printed parts. In FFF, in the last years, several studies in the literature focused on the prediction of mechanical behavior of FFF printed components. Among the others, Armillotta et. al. [3] presented an empirical model for warpage prediction by varying part geometry and layer thickness for acrylonitrile butadiene styrene (ABS). Watanabe et. al. [8] investigated warpage and residual stresses through simulation of polypropylene (PP) using Ansys Polyflow. Cattenone et. al. [5] investigated the impact of process parameters and modeling choices (e.g. mesh size, material model, time step size) on simulation outcomes using Abaqus for ABS filament. Croccolo et. al. [9] proposed an analytical model to predict the strength and the stiffness properties based on input parameter variations for FFF of ABS.

There are some references in literature on FEA studies of part distortions in photopolymer-based additive manufacturing processes. Wiedemann et al. [12] developed methods to evaluate the dynamics of polymerization and shrinkage of photopolymers. Xu

et al. [13] investigated thermal stresses for shrinkages due to resin phase changes using FEA to simulate the part deformations in stereolithography.

Similarly, computational simulations of metal AM processes are being investigated by several researchers. Li et. al. [10] investigated a predictive model of part distortion and residual stress in the selective laser melting (SLM) process of AlSi10Mg using Abaqus. Song et. al. [11] used an FE-based thermomechanical model to predict the time-dependent temperature field, residual stress and resultant deformation of the Ti-6Al-4V built part using the SLM process.

In this study, the applicability of the finite element analysis simulation for the FFF printing process was investigated. A commercial software (Digimat 2019.0 from MSC Software) was used to simulate the printing process. A thermo-mechanical material model was considered for the filament material. Printed part quality was evaluated in terms of part distortion and change in dimensions. Simulation results were verified with experimental printing and measurements. The predictive simulation tool allows assessment of the printing process outcomes at the part design stage based on the part geometry, material properties, print strategy and process conditions enabling design for additive manufacturing (DfAM). For a given material, the identification of optimal processing conditions and part design enables getting the part printed right first time as opposed to the traditional approach based on experience and trial-and-error method.

2.2 MATERIALS AND METHODS

2.2.1 Design of Experiments and Digimat Simulations

A DOE based on Taguchi L9 matrix was set up to understand the influence of critical process parameters on final part properties, specifically warpage. The three process parameters being print speed, extrusion temperature and layer thickness. Three levels of these critical input parameters were selected based on the suggested ranges for commercially available ABS material and are shown in Table I. Other print parameters such as extrusion width, extrusion multiplier, infill pattern etc. were kept constant throughout all the DOE experiments. Two different geometries with triangular cross-section, one with equal width sides and one having sides with different widths were designed in Solidworks and converted into .stl format. The geometry and dimensions of the DOE test samples are shown in Figure 1. The central purpose of including the geometry with different thickness sides is to understand and quantify the effect of variation in cross-sectional widths on the warpage in final printed parts. Additionally, both these geometries provide ease of dimensional and visual analysis.

Table 1. Taguchi L9 based DOE.

DOE no.	Temprature (in °C)	Speed (in mm/s)	Layer Thickness (in mm)
1	220	20	0.15
2	220	30	0.2
3	220	40	0.25
4	230	20	0.2
5	230	30	0.25
6	230	40	0.15
7	240	20	0.25
8	240	30	0.15
9	240	40	0.2
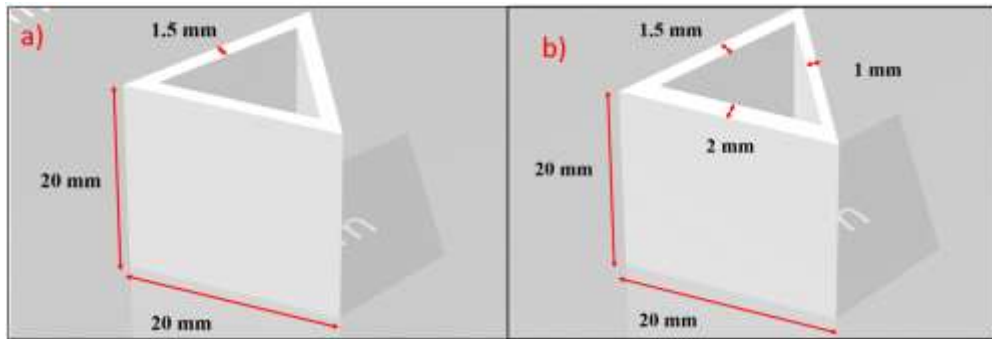
Figure 1. .stl images a) Geometry 1, b) Geometry 2

To simulate the FFF printing process, a finite element analysis (FEA) was conducted using commercial software, Digimat from MSC Software. To simulate the exact

print process, Digimat requires the material, part geometry, printer configuration and G-Code data as input. GCode determines all of the printer settings including print speed, bed temperature, cooling etc. as well as the path followed by the nozzle during a print process. The GCode was generated using the Slicer feature in an open source software called Repetier. Figure 2 shows the Digimat input section and the sliced files obtained from Repetier. Following the information in the GCode obtained from the slicing tool and the material model provided to the software, a sequential thermo-mechanical simulation was performed. The analysis was divided into two steps. First, a thermal analysis was conducted, solving a three-dimensional transient heat transfer equation to evaluate the time-spatial temperature field evolution during the printing process. The bottom surface of the model which was in contact with the platform was set to be at a constant build plate temperature. Subsequently, the resulting temperature-induced thermal strains were adopted as loading input in a mechanical analysis to evaluate residual stresses and part distortions. The mechanical analysis used a static structural analysis (elastic stress equilibrium) approach with induced thermal strains. For the mechanical boundary conditions, the bottom surface of the part was fully constrained. As per the toolpath defined by GCode instruction, a chunk of elements representing a small part of geometry was activated in each time step to mimic the continuous filament depositions action in FFF [14]. Once all the elements were activated, the results were then used for a thermomechanical analysis to simulate the solidification and cooling phase. Once the simulation finishes, the software outputs the results in the form of warpage, print time and the stress distribution both visually and numerically. For this study, the data for warpage and print time was collected and compared with actual prints.
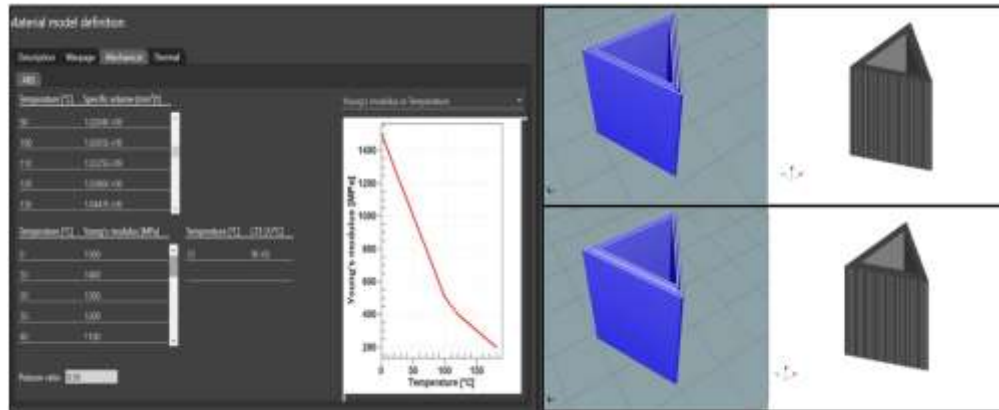
Figure 2. (left) Representative image for Digimat input section for material mechanical properties;(top right) representative images for sliced geometry and meshed geometry(from left to right)for design 1;(bottom right) representative images for sliced geometry and meshed geometry(from left to right)for design 2.

The simulation data for the Taguchi design-based DOE was then analysed using Minitab software to generate main effects plot. The main effects plot data was then used to determine worst and best possible combination of process parameters in terms of warpage and print time. To further validate the results, ANOVA analysis was performed on the generated data to determine the extent of significance of the involved factors by calculating p-values and % contribution.

2.2.2 3D Printing of DOE Samples

Commercially available ABS filament was used to print the samples on a desktop 3D printer named Makergear M2 using a 0.5 mm nozzle. All the print parameters except those included in DOE were kept constant to ascertain that only the effects of involved parameters were being monitored. After Printing, the print duration was recorded for each

sample and optical images were taken. Figure 3 shows the 3D printed parts for both the geometries. These optical images were analysed by superposing over the original models to determine the warpage values for in the printed samples.

(a)

(b)
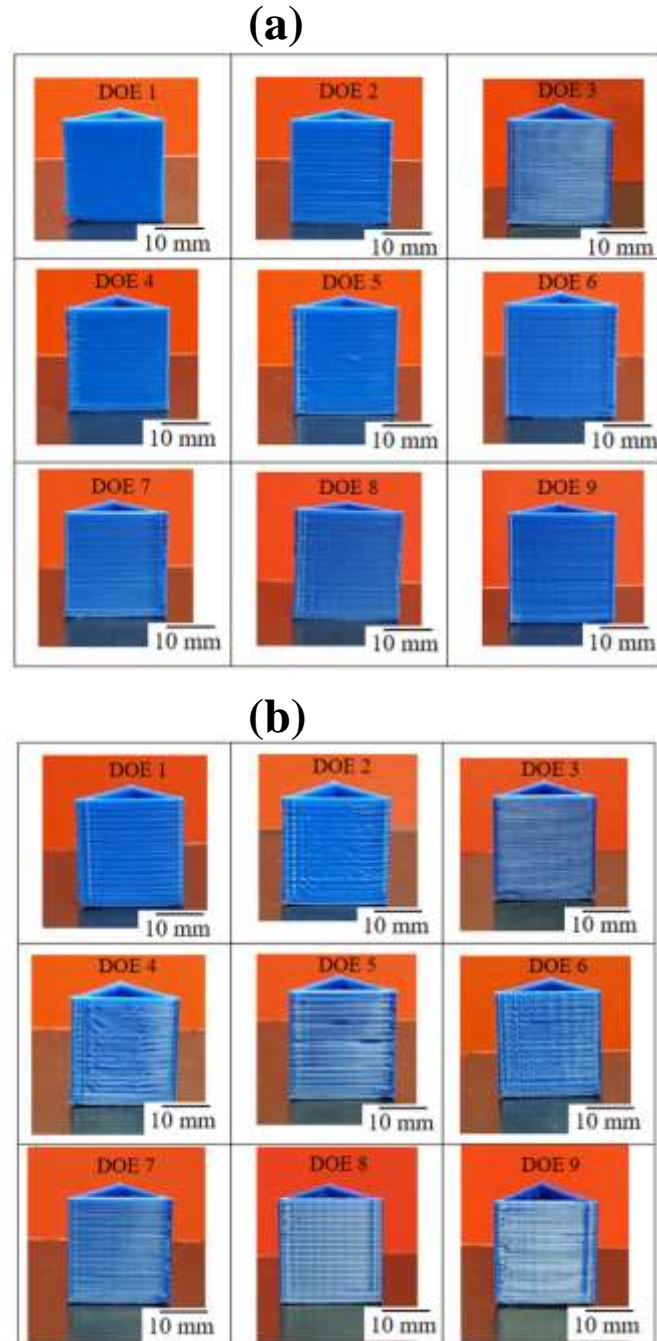
Figure 3. 3D printed ABS parts for nine DOE experiments a) Geometry 1, b) Geometry 2

2.3 RESULTS AND DISCUSSION

2.3.1   Simulated and Experimental Warpage

Figure 4 and Figure 5 show the Digimat simulation and experimental warpage comparisons between *Geometry 1* and *Geometry 1* for all nine DOEs. It can be noted that *Geometry 2* has higher warpages than *Geometry 1,* and this difference in the warpage can be attributed to *Geometry 2* having variation in wall thicknesses. For all nine DOEs and both geometries, the warpage range is between 0.3 mm to 0.41 mm. Additionally, for DOE 1 in *Geometry 1* conducted at the process parameter of 220°C, 20 mm/s, 0.15 mm had the most warpage of 0.40 mm. In contrast, DOE 3 at process parameters of 220°C, 40 mm/s, 0.25 mm has the least warpage of 0.31 mm. Parts printed for DOE 1 and DOE 3 had the same print temperatures, but the difference in print speed and layer thickness had the most significant effect on obtained warpages. Specifically, DOE 1 has the lowest speed and layer thickness combination and resulted in parts with the highest warpage. In contrast, DOE 3 has the maximum print speed and layer thickness combination between all the nine experiments and resulted in the lowest warpage values. Further sections discuss in more detail about the Taguchi analysis conducted on the warpage results.

The same nine experiments L-9 Taguchi experiments were conducted on *Geometry 2* to evaluate if print parameters have any different effects on the same geometry with variations in wall thicknesses. As observed from Figure 4, DOE 1 with the process parameter of 220°C, 20 mm/s, 0.15 mm had the most warpage of 0.41 mm. In contrast, DOE 3, with process parameters of 220°C, 40 mm/s, 0.25 mm, resulted in the least warpage of 0.32 mm, which is similar to *Geometry 1* with a slight increase in warpage. Another observation

made from the simulation results was that that warpage mostly occurred at the corners and vertical walls for both geometries. Additionally, for *Geometry 2*, most warpages were happening at the junction between the two thinnest walls for most of the DOE experiments (Figure 5).
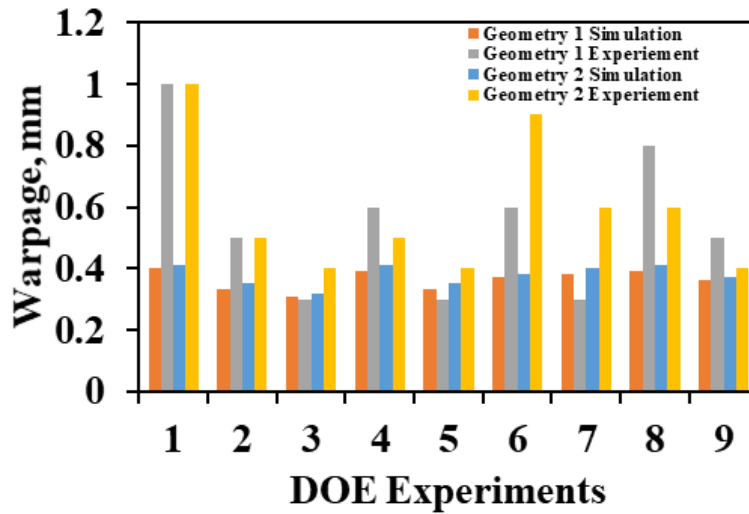
Figure 4. Simulation warpage comparison between Geometry 1 and Geometry 2

To better understand how the simulation warpage numbers represent experimentally, the FFF 3D printer resolution was considered. The printer used to print the parts had a resolution of ±0.3 mm, which provides which, when compared with the simulation warpage results, indicates that any warpage values of ~0.3mm and below can be attributed to the printer resolution and only warpages beyond 0.3 mm can be considered significant. This is a limitation of the 3D printer, and at the same time, the simulation software cannot predict the limitations of 3D printer resolution.
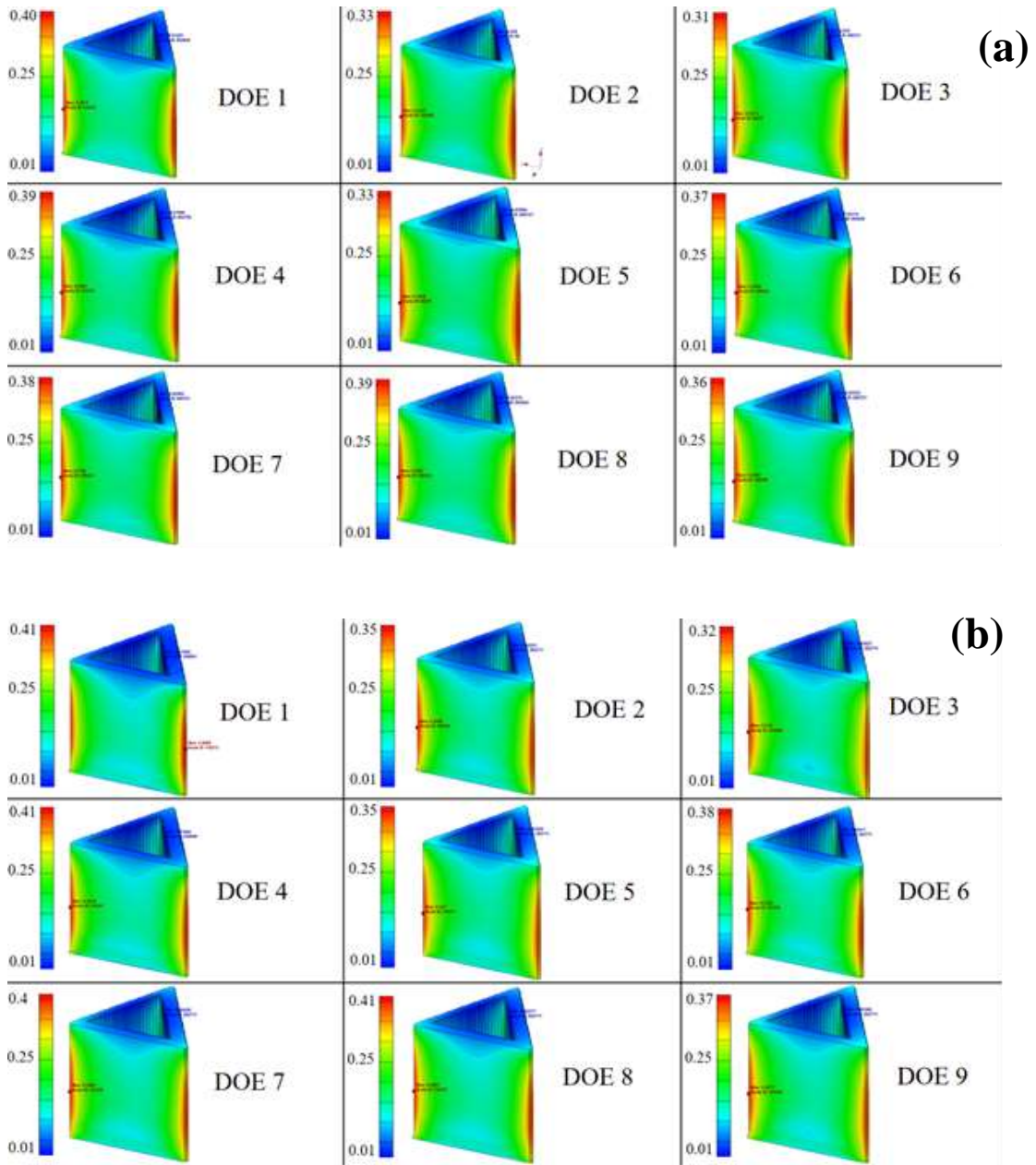
Figure 5. Digimat simulation warpage for a) Geometry 1, and b) Geometry 2

2.3.2   Simulated and Experimental Print Time

The time required to print a part is denoted here as print time. Figure 6 shows the influence of process parameters and geometry on simulated and experimental print time. Overall, the differences in print time between the Digimat simulated and the actual experimental print time for both the geometries follows the same trend with print time for *Geometry 1* is always less than that of *Geometry 2*. A more close look at DOE 1, which required the most amount of time to print, comparison between simulated and experimental printing time indicates that the simulated print time was ~20 min while the experimental print time was ~22 min for Geometry 1. A similar observation was observed for Geometry 2 with not only 2 min variation between the simulated and experimental print times, indicating that Digimat can be used to predict print times.

Lowest print time was observed in DOE 3, which had the fastest print time due to its process settings of 220°C, 40 mm/s, 0.25 mm which, when compared to DOE 1, had process conditions of 220°C, 20 mm/s, 0.15 mm. Additionally, a possible explanation for a higher print time values for Geometry two can be attributed to the variation of wall thickness (0.2, 0.15, and 0.1 mm) while the wall thickness for Geometry 1 being 1 mm constant. In contrast, the difference in print time values between experiments and simulation can be attributed to Digimat simulation does not simulate travel time from its origin point to the printing start point.
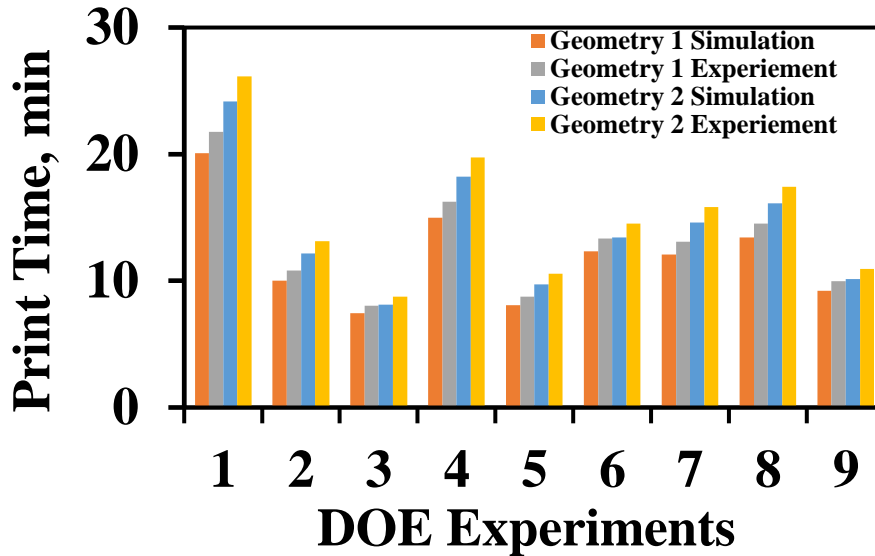
Figure 6. Print time comparison between Geometry 1 and Geometry 2 for a print time in simulation and print time experimentally

Taguchi analysis was performed on the Digimat warpage simulation results to find out how each process parameter contributes to the overall warpage of *Geometry 1* and *Geometry 2*. Additionally, comparing the warpage range between *Geometry 1* and *Geometry 2,* the same trend is observed, but variation in wall thickness tends to provide higher warpages as observed for Geometry 2. Based on Figure 7, we see that layer thickness (LT) and print speed have the most effect on the ensuing warpage for both geometries. As observed in Figure 7a for *Geometry 1*, the warpage ranged from 0.345 to 0.390 mm for print speed range from 20 mm/sec to 40 mm/sec, indicating that faster speed showed less warpage compared to a slower speed. Similarly, as observed in Figure 7b for Geometry 2, the warpage range is from 0.355 mm to 0.40 mm for speed range from 20 mm/sec till 40 mm/sec, faster speed showed less warpage compared to a slower speed.

Additionally, Figure 7a shows the trend for the warpage due to LT being similar to print speed, and it ranged from 0.34 mm to 0.38 mm. In contrast, the temperature has the

17

least effect on the warpage as it had a warpage range from 0.345 mm to 0.375 mm. A similar trend was observed for Geometry 2, as shown in Figure 7b. Layer thickness (LT) effect's on the warpage are similar to speed; it has a warpage range from 0.355 mm to 0.395 mm. The temperature has the least effect on the warpage as it had a warpage range from 0.36 mm to 0.39 mm.

Based on Figure 7, we found that the optimal process parameters for printing ABS are the lowest warpage conditions of 220°C print temperature, 40 mm/s, print speed, and 0.25 mm layer thickness. While the worst printing process parameter that results in the maximum warpage is 240°C print temperature, 20 mm/sprinted, and 0.15 mm layer thickness. The above best and worst print conditions were further used to take a closer look at the warpage results. Figure 8 shows printed parts with areas where the warpage occurs and comparative simulation images showing red regions with maximum warpage areas. Figure 8 results indicate a close comparison in warpage prediction between simulations and experiments.
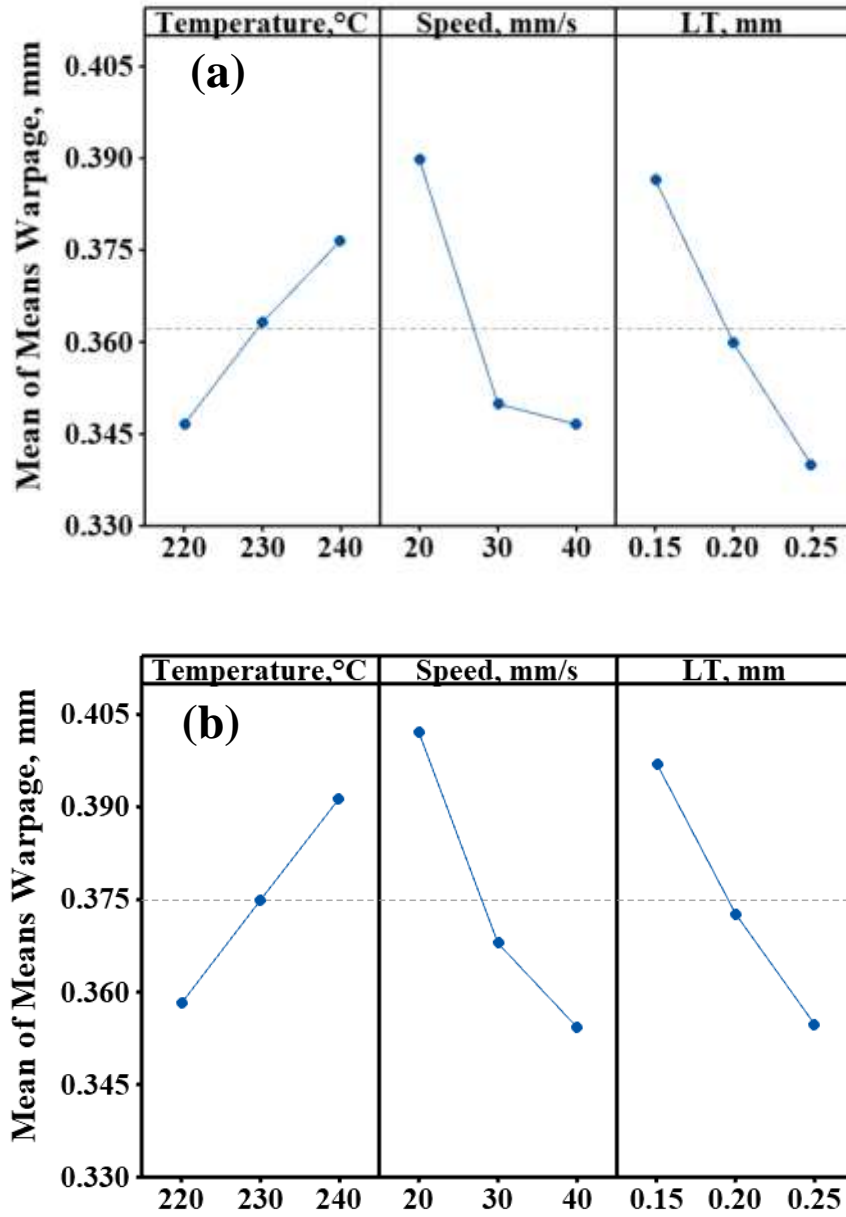
Figure 7. Main effects plot for warpage a) Geometry 1, and b) Geometry 2
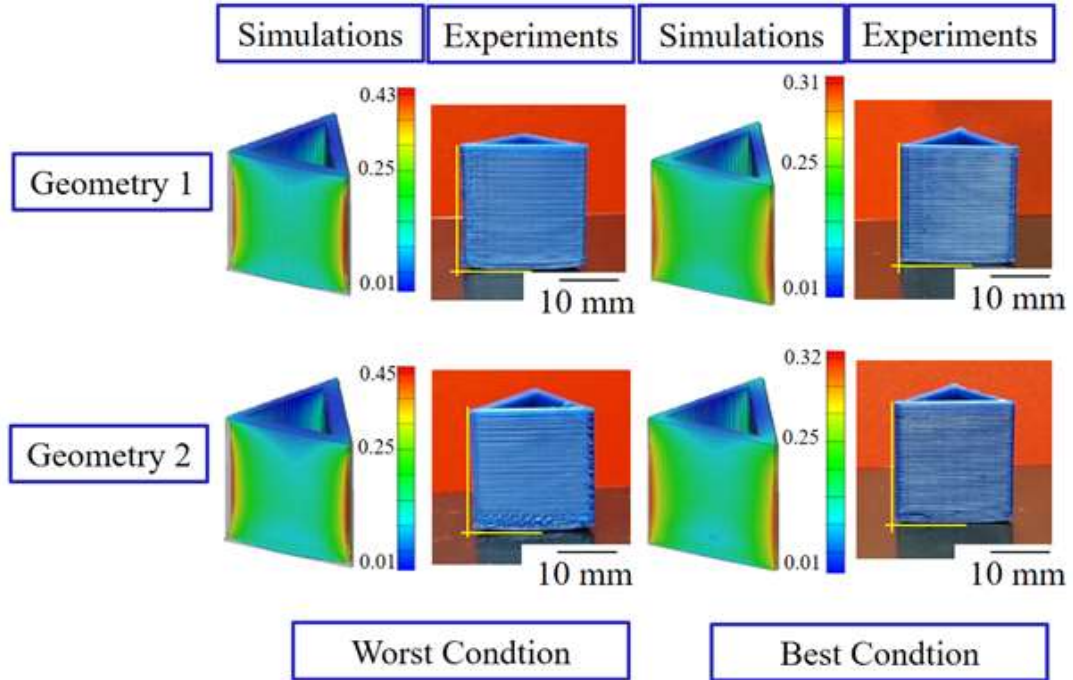
Figure 8. Print simulation and experiments showing warpage areas for best and worst print conditions for ABS FFF 3D printing

The ANOVA analysis results were used to determine the ranking of each process parameter for warpage and print time in *Geometry 1* and *Geometry 2*. Table 2 shows that for both geometries, all P-values for print temperature, print speed, and layer thickness were significant and below 0.05. Therefore, Equation 1 was used to calculate the percent contribution of each process parameter to decide the contributing ranking for print time and warpage. Table 2 provides % contribution for each process parameter and geometries.

$$\%Contribution = (Adj.Sum\ of\ Squares)/Total * 100 \qquad (1)$$

Table 2. P-value & % contribution for process parameters in Geometry 1 & 2.

		Print Temprature, °C		Print speed, mm/s		Layer Thickness, mm	
		P-Value	% Contribution	P-Value	% Contribution	P-Value	% Contribution
Geometry 1	Warpage	0.0160	16.6	0.006	42.8	0.007	40.6
	Print Time	0.507	1.1	0.022	51.7	0.0250	47.2
Geometry 2	Warpage	0.005	20.6	0.002	45.6	0.003	33.8
	Print Time	0.497	1.3	0.021	58.4	0.031	40.3

For *Geometry 1*, Table 2 indicates that print speed had the most effects on the warpage at a 42.8% contribution followed by layer thickness at 40.6% contribution, followed by the print temperature at 16.6% contribution. Additionally, Table 2 indicates that print speed had the most effects on the print time with the highest % contribution of 51.7,% followed by layer thickness at 47.2%. However, print temperature % contribution to print time can be neglected as it was ~1%.

Similarly, for *Geometry 2*, Table 4 indicates that print speed had the most effects on the warpage at a 45.6% contribution followed by layer thickness at 33.8% contribution, followed by the print temperature at 20.6% contribution, which is slightly different from *Geometry 1* as we noticed an increase in % contribution for print speed and temperature and slightly decrease in layer thickness % contribution. Additionally, Table 4 indicates that print speed had the most effects on the print time with the highest % contribution of 58.4,% followed by layer thickness at 40.3%. However, print temperature % contribution to print time can be neglected as it was ~1%.

2.4 Summary

Digimat simulations can be used to predict warpages and print time for ABS. Any geometry variation such as change in wall thickness doesn't affect simulation predictions when compared with experiments. However, variations in wall thickness increase warpage and print time as indicated by simulation and experimental results. However, simulations failed to incorporate printer resolution within simulation predictions, thereby, always overestimating warpages when compared to actual experimental results. Although p-values indicate that all process parameters are significant for both warpage and print times, but calculated % contributions provide much better insight on the actual significance of the involved parameters. Print speeds have the highest contribution in affecting warpages followed by layer thickness. However, print temperatures, if within the suggested ranges, do not have a significant effect on the warpages and print times

CHAPTER 3

THERMOMECHANICAL PROPERTIES OF SOYHULL FIBERS REINFORCED ABS
COMPOSITE MATERIAL ESTIMATIONS IN DESIGN FOR FUSED FILAMENT
FABRICATION (3D PRINTING)

3.1 INTRODUCTION

Fused filament fabrication is a 3D printing process that uses a continuous filament
of a material. Filament's materials are mainly thermosets or thermoplastic materials like
(ABS, Nylon, PLA, TPU..etc..). more advanced material composites with carbon fibers or
glass fibers have shown enhanced mechanical properties. But the higher cost of carbon
fibers and glass fibers is one of the drawbacks compared to natural fibers like the fibers
extracted from Soybean hulls.

Soyhull fibers are extracted from the soybean hulls through a complex chemical
hydrolyzation process. This process is repeated and done in stages to get better pure fibers
from the soybean hulls.

Soyhull fibers are dry blended with ABS pellets and fed into the hopper of the extruder.
Unlike conventional composite extrusion where a pelletizing step is required to ensure the
proper mixing of fibers and polymer, in the current approach pelletizing step is removed.
Instead, a melt pump is added to the extruder which increases the residence time of the

mixture. This approach has resulted in good quality filament production while saving time and effort by reducing the number of steps.

The filament thus extruded passes through a water bath to cool down, then moves through stock rollers before being winded on a spool and ready for 3D printing. To ensure that the filament produced has a diameter suitable for 3D printing, a laser micrometer is used in the extrusion process to monitor the diameter on-line. This results in filaments with diameter 1.75$\pm$0.03 mm, which is the standard size of 3D printing filaments. An accelerometer has also been used for process monitoring. A correlation between the monitored vibration and the composition of the materials and the resultant filament diameter has been noticed.

The processing conditions like temperatures at different heating zones, extruder screw speed, melt pump speed, stack roller and winder speeds, etc. were optimized to ensure good quality filaments.

3D printings experiments were done with ABS filament and with the produced ABS-SFRC filaments. A thermomechanical simulation was conducted to measure the warpage associated with 3D printing of ABS-SFRC. In order to properly run thermomechanical simulations the material properties of ABS-SFRC were calculated in this work like density, thermal conductivity, specific heat, modulus, coefficient of thermal expansion, and specific volume.

3.2 MATERIALS

3.2.1 Hydrolyzed soyhull fibers

Soyhulls are processed in two stages of hydrolysis. In the first stage the collected hydrolysate contains primarily arabinose. The collected hydrolysate for the second stage contains primarily xylose which will be further concentrated. The resulting hydrolyzed biomass is then dried with ethanol and used in making the 3D printing filaments.

Figure 9. (a) Soyhulls after Stage I (left picture), and (b) soy hulls after Stage II (right picture).

3.2.2 Thermomechanical properties

Many different approaches to calculate composite material property has been identified in research and literature. But calculating the composite property requires identifying the individual property for each component. Virgin Polymers have standard properties while the natural fibers (Soyhull fibers) do not have standard measured properties. Trying to identify these properties experimentally is costly and time consuming while in general natural fibers have typical chemical and microcrystallinity structure which means their mechanical and thermal property is relatively similar to each other.

Properties of the soyhull fibers were estimated form literatues. The fiber properties from literature are for microcrystalline cellulose and were used along with the ABS properties to get the composite material properties needed for the thermomechanical modeling in Digimat. Composite property was calculated using various models that can predict material property of mixtures.

Table 3. Mechanical and Thermal Property of Soyhull fibers.

Property	Value	Reference
Density, g/cm^3	1.50	Experimentally determined
Specific heat, J/kg k	882	[19]
Thermal conductivity, mW/mm °C	0.17	[19]
Coefficient of thermal expansion, 1/°C	1.83*10^-5	[16-18]
Modulus, Mpa	25000	[20]

Digimat standard ABS material properties at room temperature was extracted from Digimat 2021 databases.

Table 4. ABS materials properties

26

Property	Value
Density, g/cm^3	1.03
Specific heat, J/kg k	1.30E+09
Thermal conductivity, W/m °C	0.18
Coefficient of thermal expansion, 1/°C	9.00E-05
Modulus, Mpa	1300

Mechanical and Thermal properties of composite material are calculated based on Soyhull and ABS thermomechanical properties individually following different models utilized by different literature.

Specific Volume

Specific is volume is essential in providing information of how material warpage occurs for different material composite. ABS-SFR composite's specific volume would provide essential information of the material at different temperatures.

The specific volume was calculated using the rule-of-mixtures [23].

$$v_c = X_p v_{\,p} + v_f \left(1 - X_f \right) \qquad \textbf{Equation 1}$$

where, v is the specific volume, X is the mass fraction of the polymer and the subscripts c, p and f refer to the composite, polymer and filler respectively.
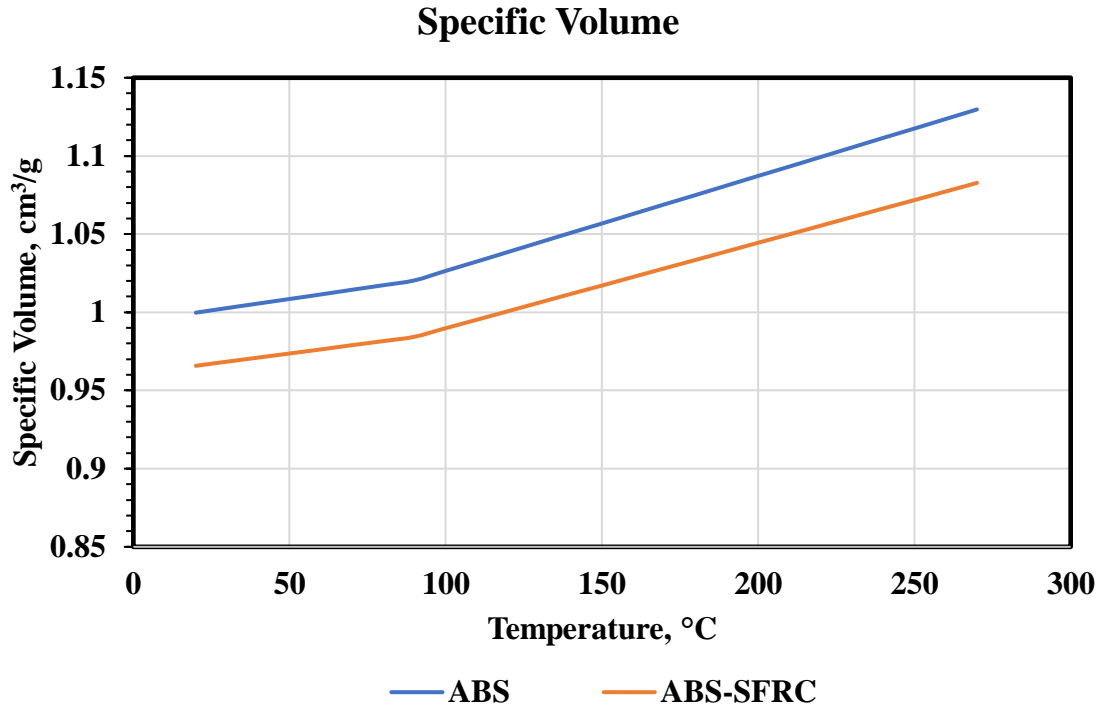
Specific Volume

Figure 10. Specific volume for ABS and ABS-SFRC materials at different temperatures

Specific volume for ABS and ABS-SFRC is shown in figure 10 at different temperatures. The difference between ABS and ABS-SFRC specific volume is not large since only 10% of fibers are included in the mixture.

Young's modulus

The Young's modulus of the composite material is essential in determining the strength and distortion of 3D printed geometries using FDM process. Among various models available to predict the Young's modulus of a powder-polymer mixture, Halpin and

Tsai developed a widely accepted model which takes into account the filler shape and size. This model is as shown in Equation 2 [20].

$$\frac{E_c}{E_p} = \frac{1+\xi\eta\phi_f}{1-\eta\phi_f}$$ **Equation 2**

where, E is the elastic modulus, ξ is a shape parameter dependent on the geometry and loading direction, ϕ is volume fraction, subscripts f, c and p denote filler, composite and polymer.

The parameter η is given by equation 3 [20].

$$\eta = \frac{E_f/E_p - 1}{E_f/E_p + \xi}$$ **Equation 3**

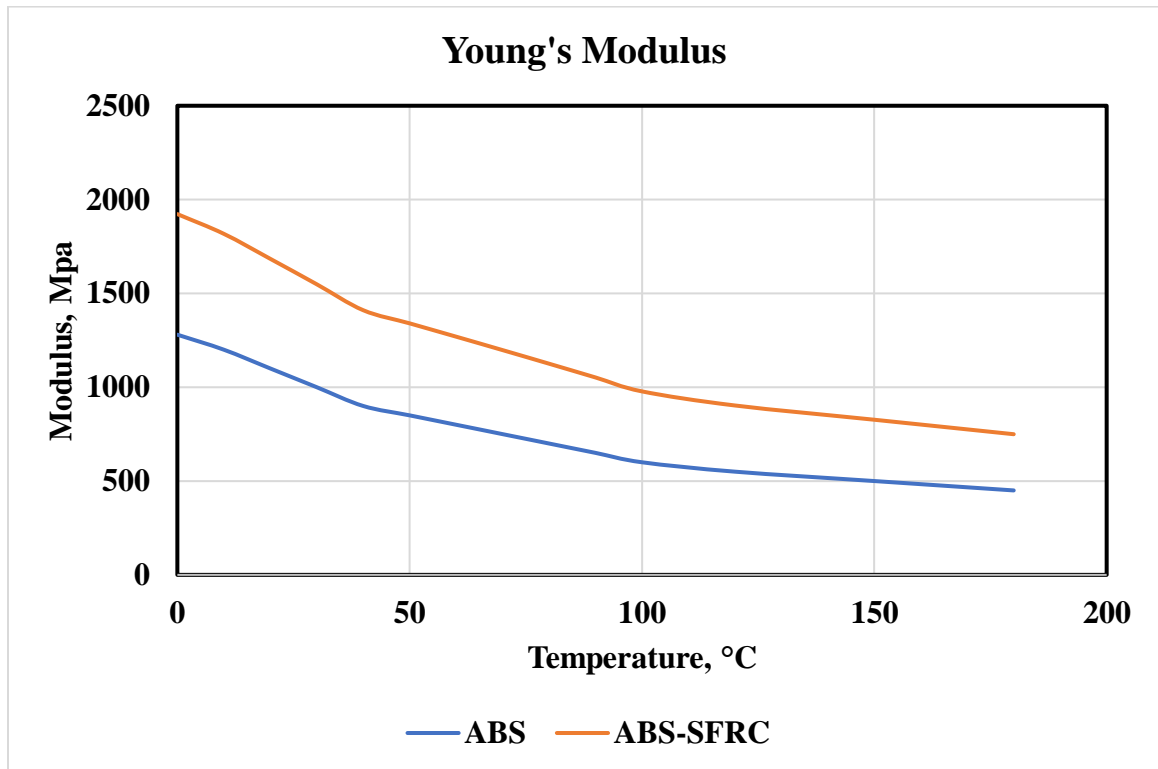The parameter, ξ can be approximated to be 10 for short fibers.

Figure 11. Young's modulus for ABS and ABS-SFRC material at different temperatures

An improvement of composite modulus has been calculated and experimentally verified by conducting tensile testing on filament produced with the composite material.

Specific heat

Thermal properties of ABS and ABS-SFRC depend on the processing temperature. For fused filament fabrication with composite material, it is essential to understand the difference in specific heat properties between pure polymers and filled polymers.

A modified rule of mixtures was used [22] as given in equation 4 below to determine the specific heat of ABS-SFRC.

$$C_{p_c} = \left[C_{p_f} X_f + C_{p_p} X_p \right] * \left[1 + A * X_f X_p \right] \qquad \textbf{Equation 4}$$

where, A is a correction factor assumed to be 0.5 for soyhull fibers. A factor of 0.2 for spherical particles was used to determine the difference on specific heat with different fiber geometries. The specific heat variance due to fiber geometry factor is very small and almost negligible.
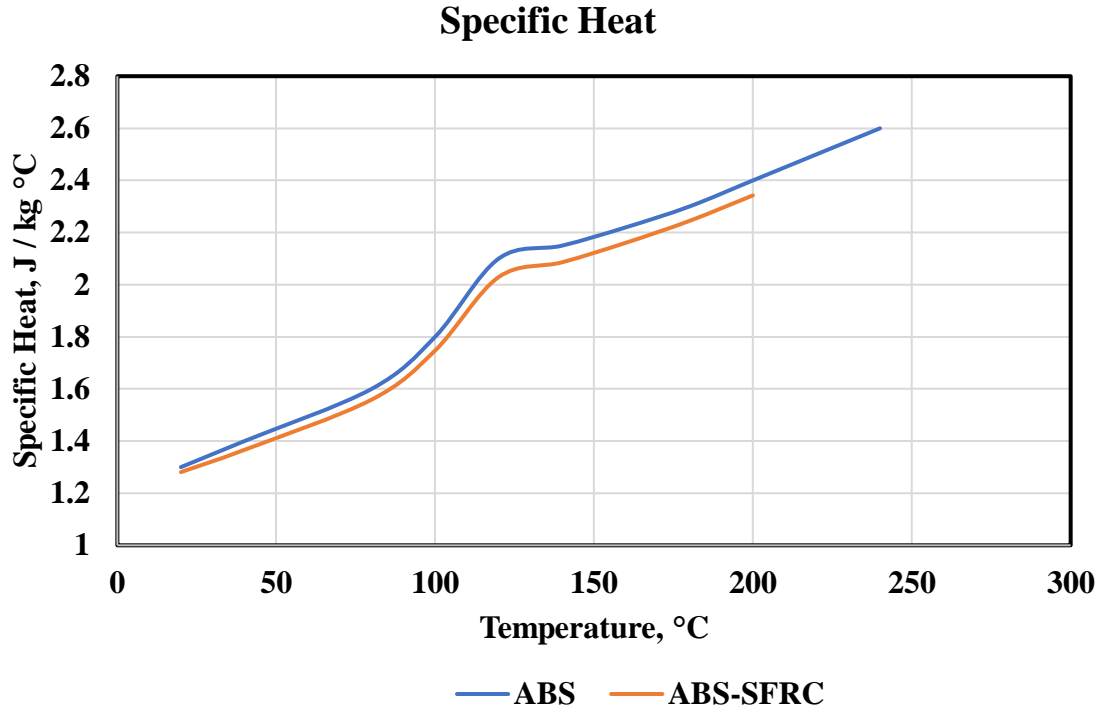
Figure 12. Specific heat for ABS and ABS-SFRC material at different temperatures

Thermal conductivity

Fused filament fabrication process depends on materials thermal properties at temperatures near to glass temperature or even at melt temperature.

Thermal conductivity of composite was measured using the rule of mixtures [23].

$$k_c = k_m \phi_m + k_f \phi_f \qquad \textbf{Equation 5}$$

Table 5. Thermal conductivity of ABS and Soyhull fiber

Thermal Conductivity W/m °C

31

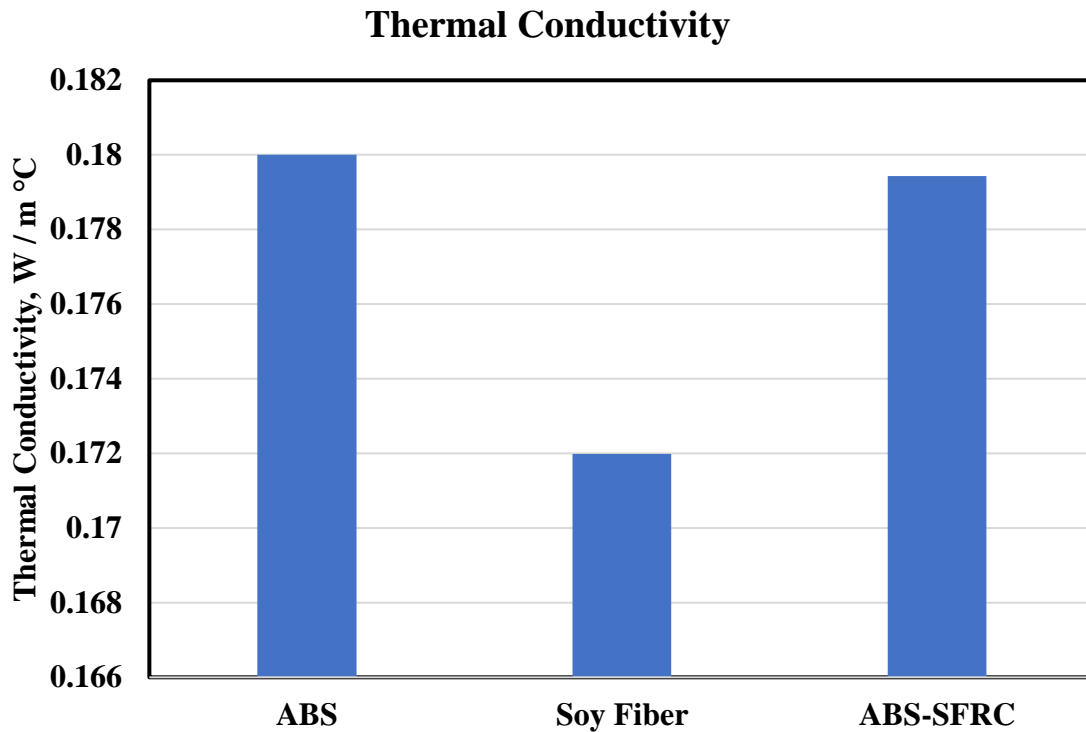| ABS	Soyhull fibers
0.180	0.170

Thermal Conductivity

Figure 13. Thermal conductivity for ABS, Soy Fiber and ABS-SFRC materials at room temperature.

Thermal conductivity of soyhull fiber reinforced ABS is slightly smaller compared to pure ABS.

Coefficient of thermal expansion (CTE)

During fused filament fabrication deposited materials expand and shrink because of the thermal cycle of the heated nozzle and the molten materials. For composite materials it is

very essential to determine CTE for the matrix and the composite. The general rule-of-mixtures is a simple approach to calculate the composite coefficient of thermal expansion per the following equation 6 [23].

$$\alpha_c = \phi_p \alpha_p + \alpha_f \left(1 - \phi_p\right) \qquad \textbf{Equation 6}$$

where, α is the thermal expansion coefficient, ϕ is the volume fraction of the polymer and the subscripts c, p and f stand for composite, polymer and filler respectively.
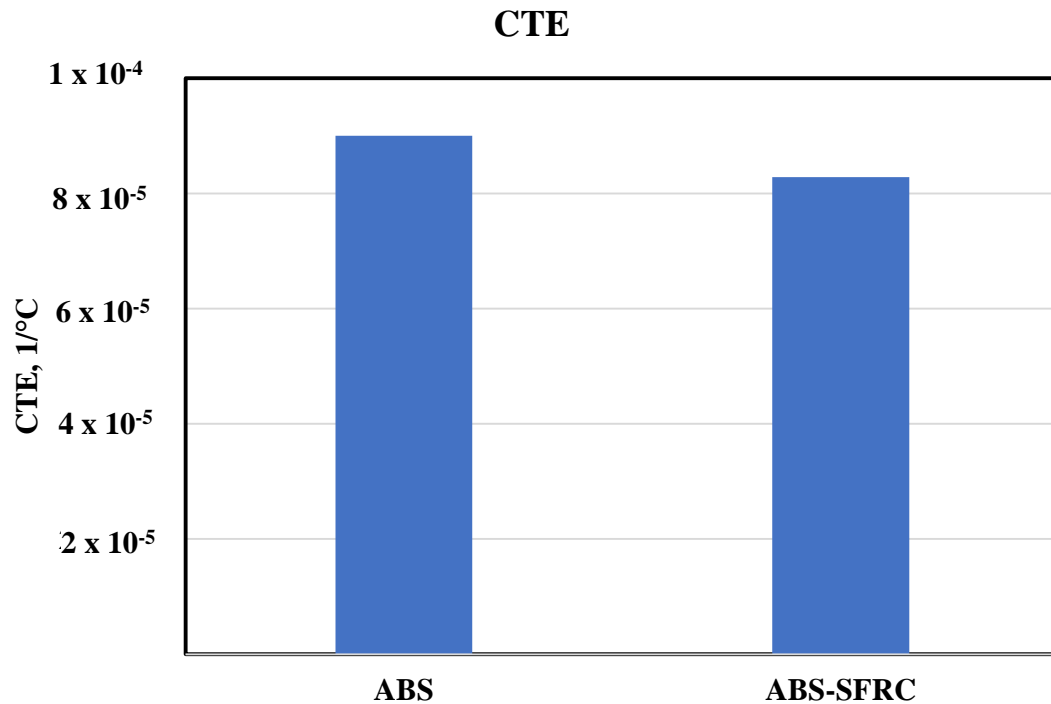

Figure 14. CTE for ABS and ABS-SFRC materials at room temperature.

3.3. EXPERIMENTS AND SIMULATIONS

3.3.1 Filament Production

Soyhull fibers reinforced ABS composite filament was produced using a filament production line which consists of single screw extruder machine equipped with a melt pump followed by a water bath for water cooling the filament below glass temperature after it exits the extruder. The filament goes through a stack rollers which applies tension on the filament through different combination of rollers for diameter control. Diameter laser measuring device is placed through the stack rollers to confirm the control of filament's diameter before it is spooled with a spooler machine at the end of the filament production line. Spools of ABS-SFRC filaments are shown in figure 16.
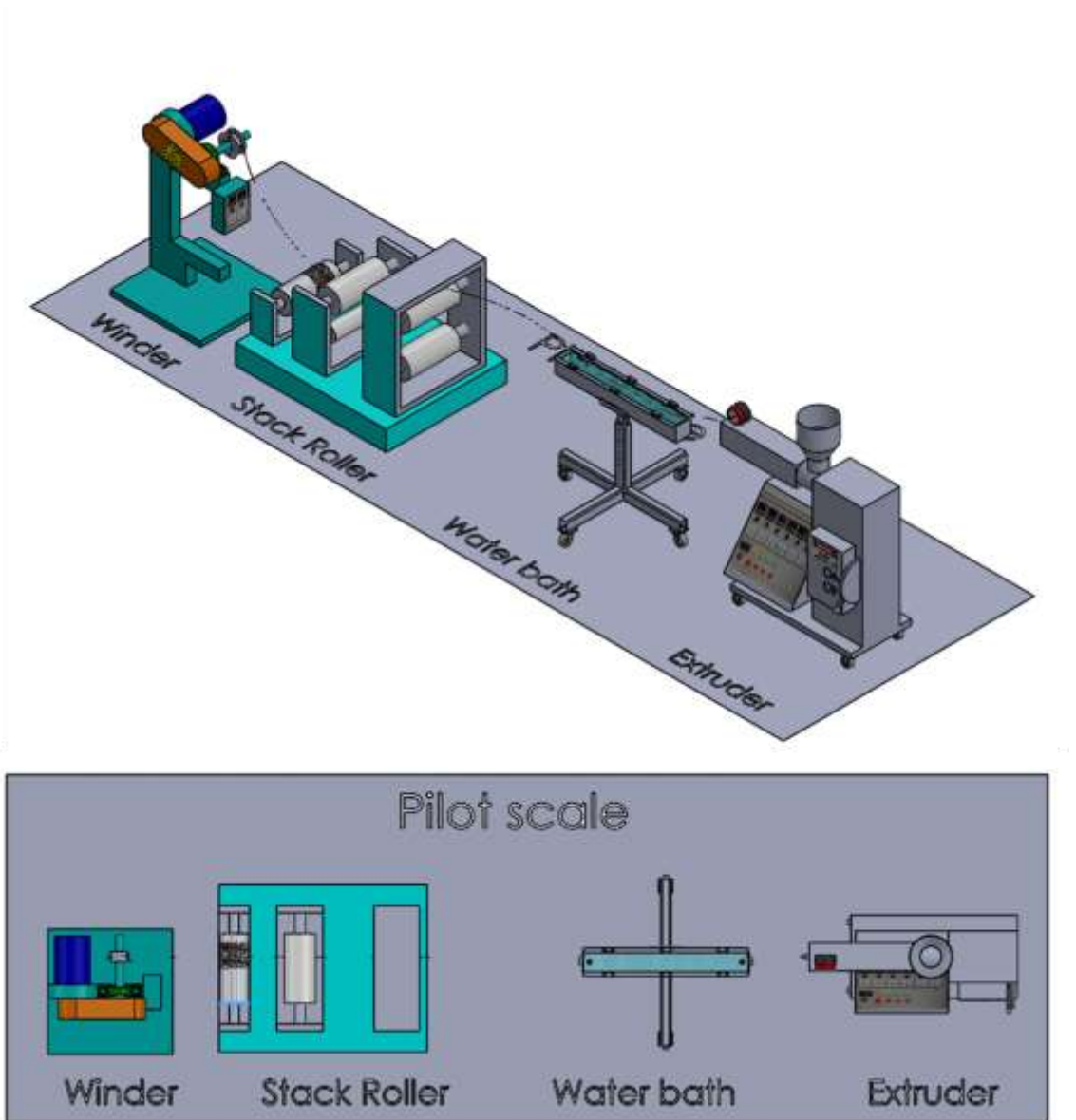
Figure 15. Filament production line schematic (Extruder, Water bath, Stack Roller and Winder)

Figure 16. Soyhull fibers reinforced polymer composite filament spools with different fiber loadings (10% & 20%)

Mechanical testing on produced filaments were conducted to evaluated its properties and compare it with mathmatically calculated material properties.

Table 6. Tensile test results for acrylonitrile butadiene styrene (Cycolac) filaments

Material	Tensile Modulus (MPa)	Tensile Stress at Break (MPa)	Tensile Strain at Break (%)
ABS	1285	24	7.9
ABS-SFRC	1467	30	4.8

ABS-SFRC with 10% fibers loading showed enhanced mechanical properties compared to pure ABS similar to the mathmatically calculated mechanical properties as we see from table 6.

3.3.2 Simulations

A DOE based on Taguchi L9 matrix was set up to understand the influence of critical process parameters on final part properties, specifically warpage. The three process parameters being print speed, extrusion temperature and layer thickness. Three levels of

these critical input parameters were selected based on the suggested ranges for commercially available ABS material and are shown in Table I. Other print parameters such as extrusion width, extrusion multiplier, infill pattern etc. were kept constant throughout all the DOE experiments.

Geometry with triangular cross-section with equal width sides was designed in Solidworks and converted into .stl format. This geometry will be used to measure warpages using Digimat simulation.

To simulate the FFF printing process, a finite element analysis (FEA) was conducted using commercial software, Digimat from MSC Software. To simulate the exact print process, Digimat requires the material, part geometry, printer configuration and GCode data as input. GCode determines all of the printer settings including print speed, bed temperature, cooling etc. as well as the path followed by the nozzle during a print process. The GCode was generated using the Slicer feature in an open source software called as Repetier. Following the information in the GCode obtained from the slicing tool and the material model calculated in the previous section of the Soy fibers filled ABS composite material provided to the software, a sequential thermo-mechanical simulation was performed.

The simulation data for the Taguchi design-based DOE was then analysed using Minitab software to generate main effects plot. The main effects plot data was then used to determine worst and best possible combination of process parameters in terms of warpage and print time.

3.3.3 3D Printing Experiments

3D printing of the worst and best process conditions identified by the Taguchi design analysis was performed to compare and validate the simulation results. Additionally comparing the 3d printed geometries with Soyhull fibers reinforced ABS was compared with geometries printed with pure ABS on chapter 1 to compared simulation and experiments results between pure ABS and Soyhull fibers reinforced ABS.

3.4. Results and Discussions

In this section the thermomechanical simulation of warpage in the composite 3D printed part and the experimental determination of warpage will be discussed.

3.4.1. Simulation Results

Based on the previous section where we have mathematically calculated the thermomechanical properties of ABS-SFRC materials. It showed better mechanical properties and better thermal properties during printing as the soy fibers have lower specific heat and thermal conductivity which should ideally result in lower warpages.

9 DOEs were analysed in Digimat for warpage prediction. Results of the 9 Digimat simulations are shown in the figure 15.
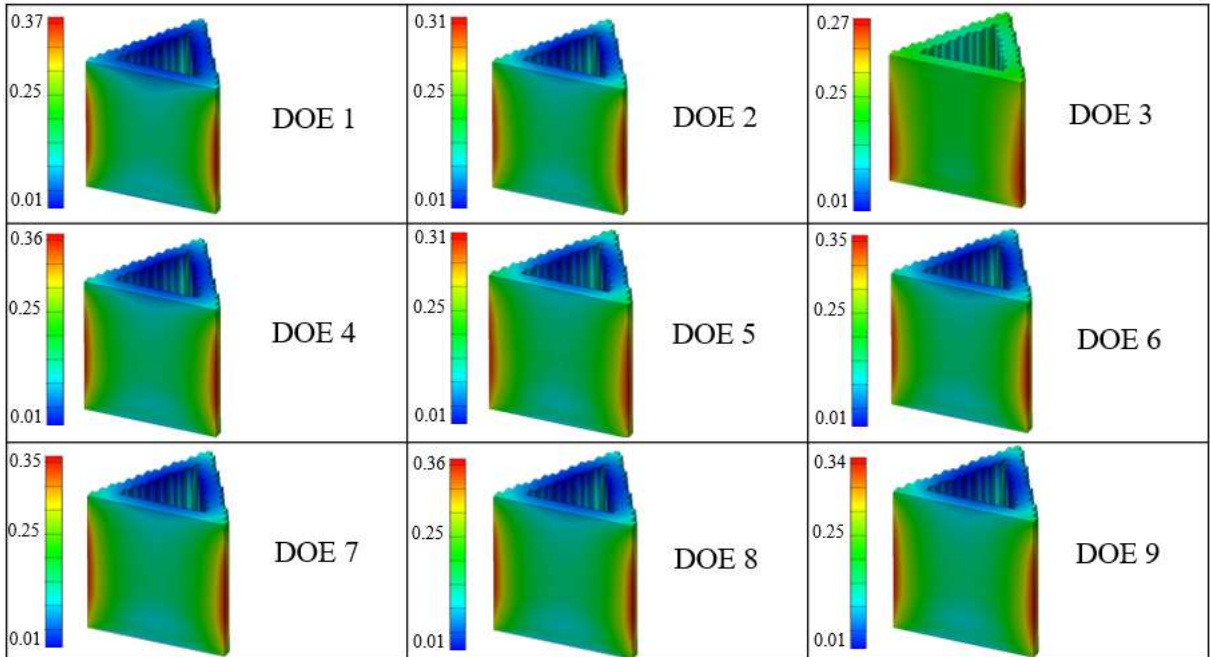
Figure 17. 9 DOE Simulation experiments with Digimat

Taguchi analysis has been conducted to evaluate the effect of every factor on the overall warpage. Temperature contribution to the overall warpage ranged from 0.33 - 0.36 mm which is the lowest range compared to other factors. Speed Contribution to the overall warpage ranged from 0.32 - 0.37 mm. Layer thickness contribution to the overall warpage ranged from 0.315 - 0.37 mm which is the highest range compared to other factors.

From the taguchi analysis the worst and best process conditions were determined.

Worst Process conditions are identified as (Temperature 240 °C, Speed 20 mm/sec and layer thickness of 0.15 mm). which is the exact worst process conditions for pure ABS. Best Process conditions are identified as (Temperature 220 °C, Speed 40 mm/sec and layer thickness of 0.25 mm). which is the exact best process conditions for pure ABS
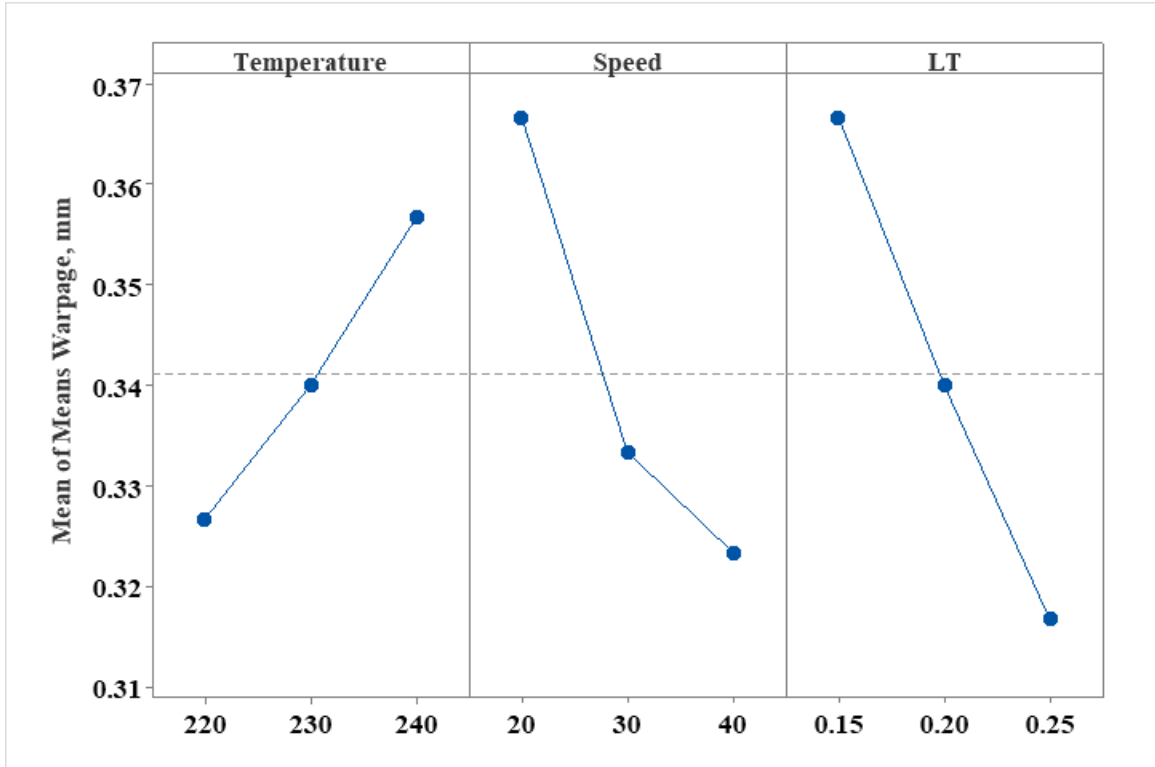
Figure 18. Warpage effects plot for Taguchi analysis

ABS reinforced with soy fiber composite showed less warpage in comparison with pure ABS. Figure 17 shows Digimat simulation warpage results comparison between pure ABS and Soybean fiber reinforced ABS composite for all 9 DOEs.
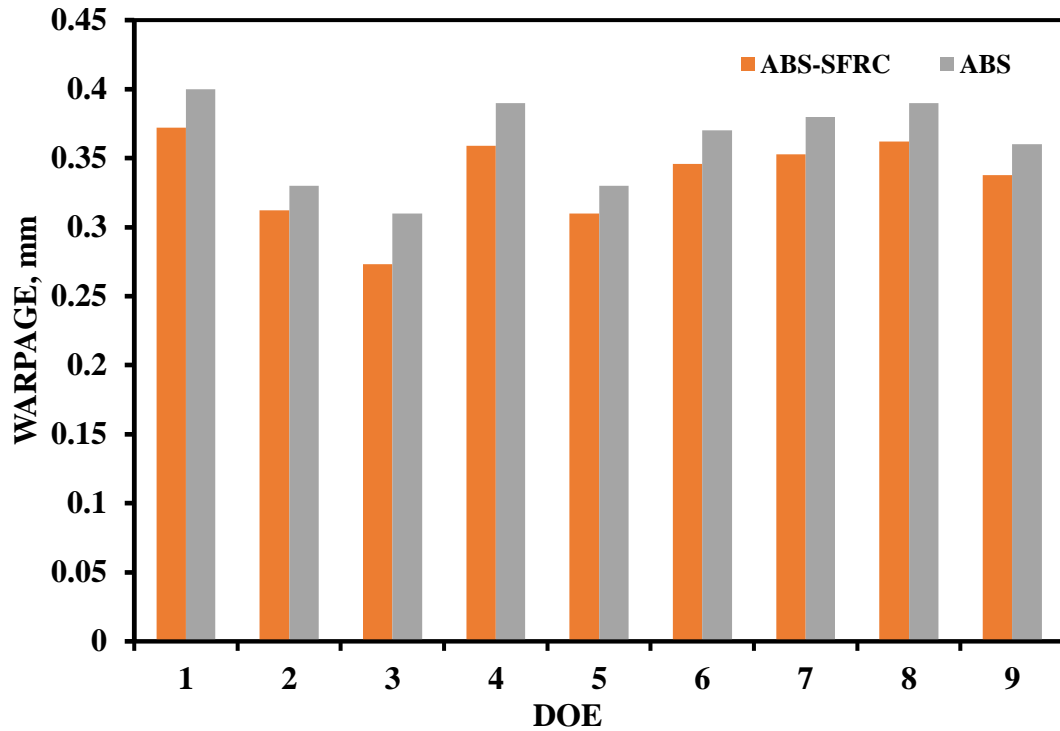
Figure 19. Warpage simulation results comparison between geometries 3D printed with ABS and ABS-SFRC

3.4.2. Experiments Results

using the ABS-SFRC filaments produced with the pilot scale production line extruder and using the worst and best process conditions identified earlier. A Digimat simulation was conducted and actual 3D printing of geometry 1 with ABS-SFRC filament has taken place with both process conditions. Simulation and experiments results are shown below.
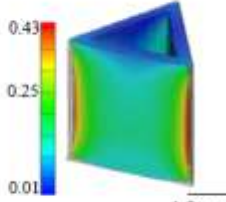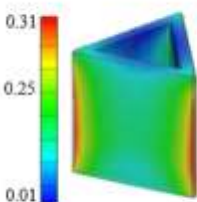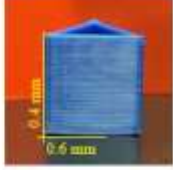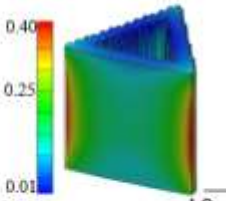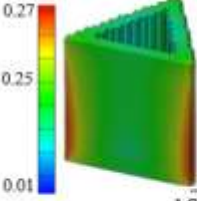
Figure 20. Print simulation and experiments showing warpage areas for best and worst print conditions for ABS & ABS-SFRC FFF 3D printing

Digimat simulation of ABS-SFRC using worst process conditions (Melt temperature 240°C, print speed 20 mm/sec and layer thickness 0.15 mm) shows a warpage of 0.40 mm. The highest warpages concentrate around the corners of the triangular geometry. Which is lower compared to the pure ABS simulated warpage of 0.43 mm.

3D printing of the actual triangular geometry with SOY/ABS filament also has less warpage compared to printed geometry with pure ABS using worst process conditions. Warpage measured experimentally for ABS/SOY printed geometry is 0.7 mm horizontally and 0.0 mm vertically. While warpage measured experimentally for ABS printed geometry is 0.9 horizontally and 1.2 mm vertically.

Digimat simulation of ABS-SFRC composite using best process conditions (Melt temperature 220°C, print speed 40 mm/sec and layer thickness 0.25 mm) shows a warpage of 0.27 mm. The highest warpages concentrate around the corners of the triangular geometry. Which is lower compared to the pure ABS simulated warpage of 0.31 mm.

3d printing of the actual triangular geometry with ABS-SFRC filament also has less warpage of actual 3d printed geometry with pure ABS using best process conditions. Warpage measured experimentally for ABS/SOY printed geometry is 0.4 mm horizontally and 0.1 mm vertically. While warpage measured experimentally for ABS printed geometry is 0.4 horizontally and 0.6 mm vertically.
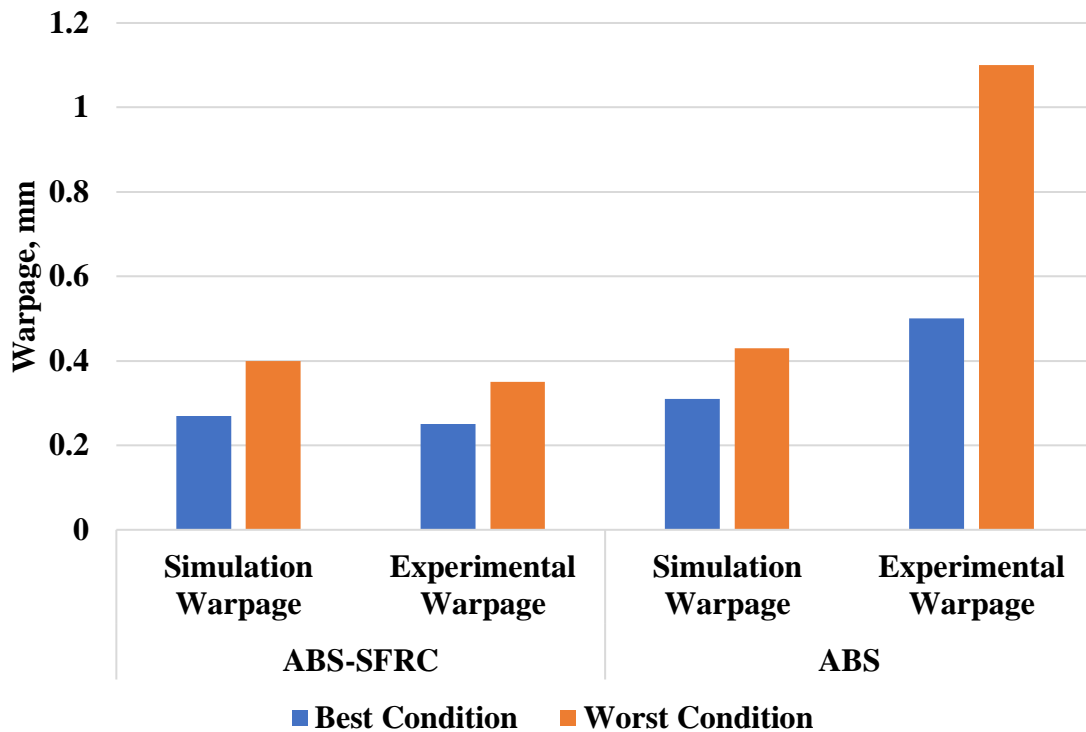
Figure 21. Warpage comparison between ABS-SFRC vs ABS printed geometry for best and worst conditions

Looking at both geometries printed with ABS and ABS-SFRC with the naked eyes. the warpage difference between them can be distinguished very easily as the ABS-SFRC geometry is not as warped at the bottom and corners compared to the pure ABS geometry
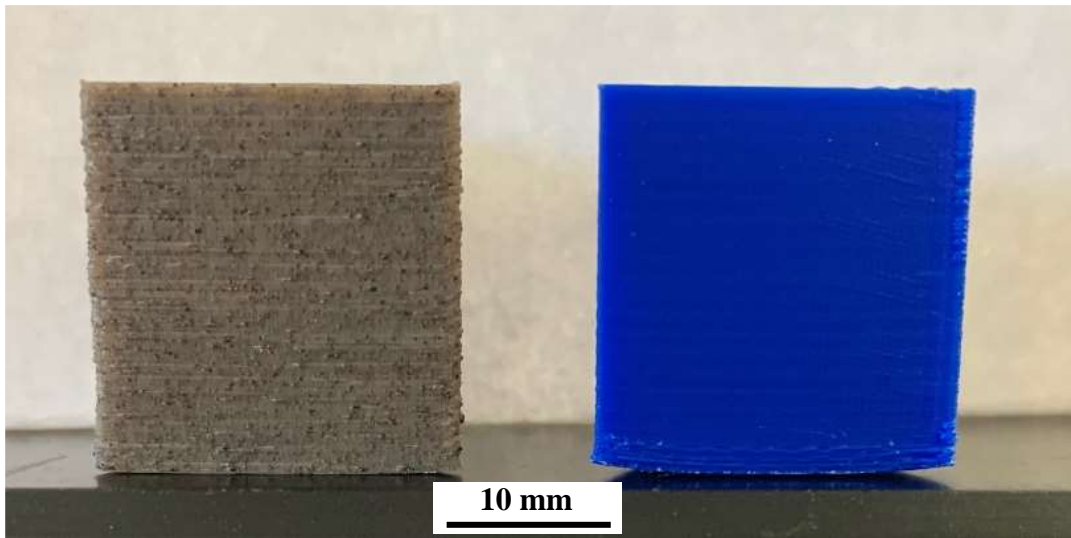
Figure 22. Side view of triangular geometries printed at worst process conditions with ABS-SFRC (left geometry) and pure ABS (right geometry)

3.5. Summary

In this work natural fiber reinforced polymer composite thermomechanical properties were experimentally and analytically tested and calculated. A thermomechanical simulations for geometries printed with ABS reinforced with soybean fibers has been conducted which proved that Natural fiber composite materials have good thermomechanical properties which lead to less warpages during printing which could lead to more potential application for the natural fiber composite materials.

Process parameter still plays an important role in the final thermomechanical property of the geometry but having a good combination of process parameters with relevant material properties leads to the most optimum application of fused filament fabricated parts.

CHAPTER 4

CONCLUSION

Fused filament fabrication is an easy fast way to produce prototype for different applications and industries like automotive and aerospace. Accuracy and resolution does not meet industry standards due to warpages formed during the thermal process in fused filament fabrication. Early identification of warpage formation is critical in order to determine process parameter selection and design modification before any 3d printing trials. Which could lead to less material waste and less energy consumption. Thermomechanical simulation can predict such warpages at an early stage before any 3d printing experiments. Different thermomechanical simulations using different process parameters were analysied. Based on the conducted thermomechanical simulations using Digimat, process parameters percentage effects on warpage were determined. Print speed is the most significant factor on warpage follwoed by layer thickness and print temperature. From the 9 different process parameters group warpage simulations, best and worst process parameter were identified. 3D printing geometries utilizing the best process parameters still results in warpage which leads to the need of developing a new composite material that is capable of being 3d printed with better accuracy and resolution.

Natural fibers reinforced composite have been utilized in many different industries like automotive and aerospace due to its lightweight and better mechanical properties using injection molding manufacturing processes. Fused filament fabrication of natural fibers

composite materials is a novel process with not much research conducted about it. soybean fibers reinforced ABS composite thermomechanical properties were experimentally and analytical tested and calculated. Thermomechanical simulations for geometries printed with ABS reinforced with soybean fibers has been conducted which showed that ABS reinforced with soybean fibers composite materials have good thermomechanical properties which lead to less warpages during printing which could lead to more potential application for the natural fiber composite materials.

İmproving the accuracy of fused filament fabricated parts is a multi dimensional approach related to geometry design, process parameter selection and material properties. Utilizing the best geometry design suitable for fused filament fabrication with optimum process parameters (Print speed, layer thickness and print temperature) relevant to the thermomechanical properties of the filament materials is the best approach to improve the 3D printed geometry resolution.

CHAPTER 5

FUTURE WORKS

Natural fibers proved to have huge benefits for many industries especially automotive and aerospace due to their lightweight and good thermomechanical properties. İmproving and developing lightweight components for automobile or airplane parts are not restricted on developing new composite materials only but also related to design aspects. Topology optimization and generative design have huge impacts on reducing the weight for automobiles and airplanes without sacrificing the performance of the parts. Merging natural fiber composite materials with generative design techniques could lead to better results and open new doors for natural fibers composite materials utilisation.

Additionaly, continous monitoring and analysis of components and parts made of natural fiber composites is a long term process and should not be restricted to initial analysis and simulations prior to additively manufacturing it. Digital twin plays an important role in monitoring the performance of actual parts and relate it to its virtual model which could lead to better design improvements and increase in lifespan of the components.

Utilizing newly developed material composites in parts manufacturing with cutting edge design technologies like generative design and digital twin simulation will open doors for new possibilities and applications for natural fiber reinforced composites.

REFERENCES

1. Gonzalez-Gutierrez, J., Cano, S., Schuschnigg, S., Kukla, C., Sapkota, J., Holzer, C., *Additive manufacturing of metallic and ceramic components by the material extrusion of highly-filled polymers: a review and future perspectives.* Materials 2018. 11(5): p. 840

2. Huang, C., *Extrusion-based 3D Printing and Characterization of Edible Materials.* UWSpace. http://hdl.handle.net/10012/12899

3. Armillotta, A., Bellotti, M., Cavallaro, M., *Warpage of FDM parts: Experimental tests and analytic model.* Robotics and Computer-Integrated Manufacturing, 2018. 50: p. 140-152

4. Zhou, Y., et al., *Temperature analysis in the fused deposition modeling process*. 3rd international conference on information science and control engineering (ICISCE). 2016. IEEE.

5. Cattenone, A., et al., *Finite element analysis of additive manufacturing based on fused deposition modeling: distortions prediction and comparison with experimental data.* Journal of Manufacturing Science and Engineering, 2019. 141(1)

6. Pennington, R., Hoekstra, N., Newcomer, J., *Significant Factors on the Dimensional Accuracy of Fused Deposition Modeling,* https://doi.org/10.1243/095440805X6964

7. Jiang, K., Gu, Y., *Controlling Parameters for Polymer Melting and Extrusion in FDM,* Key Engineering Materials, vol. 258-259, 2004, pp. 667-671

8. Watanabe, N., et al., *A model for residual stress and part warpage prediction in material extrusion with application to polypropylene*. Annual International Solid Freeform Fabrication Symposium, Austin. 2016

9. Croccolo, D., De Agostinis, M., Olmi, G., *Experimental characterization and analytical modelling of the mechanical behaviour of fused deposition processed parts made of ABS-M30.* Computational Materials Science, 2013. 79: p. 506-518

10. Li, C., et al., *Efficient predictive model of part distortion and residual stress in selective laser melting.* Additive Manufacturing, 2017. 17: p. 157-168

11. Song, J., et al., *Role of scanning strategy on residual stress distribution in Ti-6Al-4V alloy prepared by selective laser melting.* Optik, 2018. 170: p. 342-352

12. Wiedmann, B., Dusel, K., Eschl, J., *Investigation into Material and Process on Part Distortion,* Rapid Prototyping Journal, vol. 1(3), 1995, pp. 17-22

13. Xu, H., Zhang, Y., Lu, B., Chen, D., *Numerical Simulation of Solidified Deformation of Resin Parts in Stereolithography Rapid Prototyping,* Chinese Journal of Mechanical Engineering, vol. 40(6), 2004, pp. 107-112

14. e-Xstream, Digimat-AM simulation solution for Additive Manufacturing. https://www.e-xstream.com/product/digimat-am. Accessed 15 Jul 2020.

15. R. R. Rizkiansyah, Mardiyati, Steven, and R. Suratman, "Crystallinity and thermal resistance of microcrystalline cellulose prepared from manau rattan (Calamusmanan)," in AIP Conference Proceedings, Apr. 2016, vol. 1725. doi: 10.1063/1.4945525.

16. K. M. Picker and S. W. Hoag, "Characterization of the Thermal Properties of Microcrystalline Cellulose by Modulated Temperature Differential Scanning Calorimetry."

17. M. El-Sakhawy and M. L. Hassan, "Physical and mechanical properties of microcrystalline cellulose prepared from agricultural residues," Carbohydrate Polymers, vol. 67, no. 1, pp. 1–10, Jan. 2007, doi: 10.1016/j.carbpol.2006.04.009.

18. M. Beroual, L. Boumaza, O. Mehelli, D. Trache, A. F. Tarchoun, and K. Khimeche, "Physicochemical Properties and Thermal Stability of Microcrystalline Cellulose Isolated from Esparto Grass Using Different Delignification Approaches," Journal of Polymers and the Environment, vol. 29, no. 1, pp. 130–142, Jan. 2021, doi: 10.1007/s10924-020-01858-w.

19. J. Ketolainen, L. Kubičár, V. Boháč, M. Markovič, and P. Paronen, "Thermophysical Properties of Some Pharmaceutical Excipients Compressed in Tablets," Pharmaceutical Research: An Official Journal of the American Association of Pharmaceutical Scientists, vol. 12, no. 11, pp. 1701–1707, 1995, doi: 10.1023/A:1016261605023.

20. S. J. Eichhorn and R. J. Young, "The Young's modulus of a microcrystalline cellulose," 2001.

21. Wu, W., et al., *Predictive modeling of elastic properties of particulate-reinforced composites.* Materials Science and Engineering: A, 2002. **332**(1-2): p. 362-370.

22. Mamunya, Y.P., et al., *Electrical and thermal conductivity of polymers filled with metal powders.* European Polymer Journal, 2002. **38**(9): p. 1887-1897.

23. Kate, K.H., et al., *Predicting powder-polymer mixture properties for PIM design.* Critical Reviews in Solid State and Materials Sciences, 2014. **39**(3): p. 197-214.

APPENDICES

APPENDİX A: 3D PRINTING STUDIES

A 0.75 mm nozzle was used on FDM 3D printers to demonstrate the printability of the

composite filaments. Standard geometries like tensile test and tear test specimens were

printed for mechanical characterization. In addition, potential products were printed.

Figure 23. 3D printed parts with Soybean fibers filled HYTREL using FFF printers

Figure 24. 3D printed bike parts with Soybean fibers filled HYTREL using FFF printers

Figure 25. 3D printed parts with recycled Soybean fibers filled HYTREL
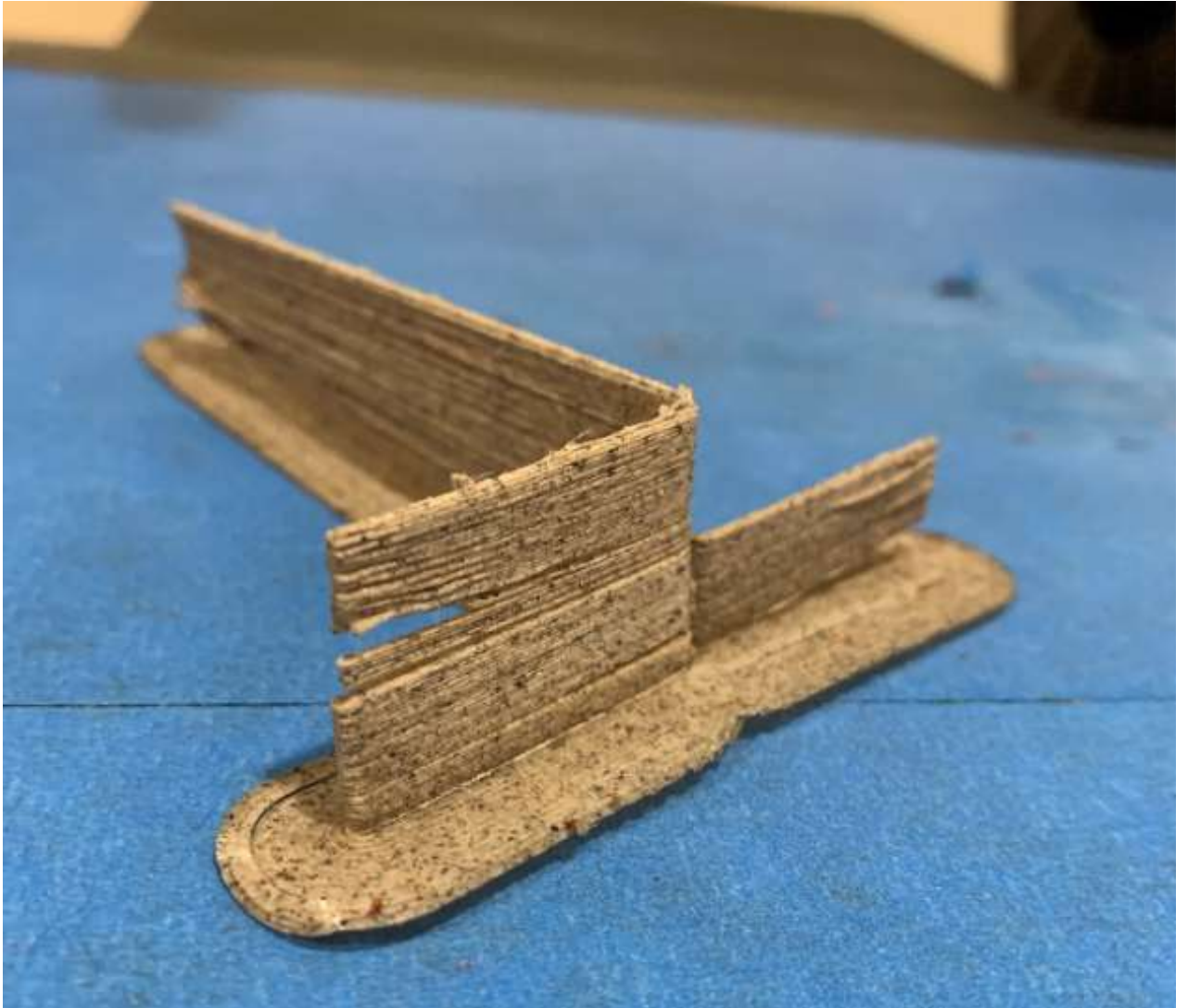
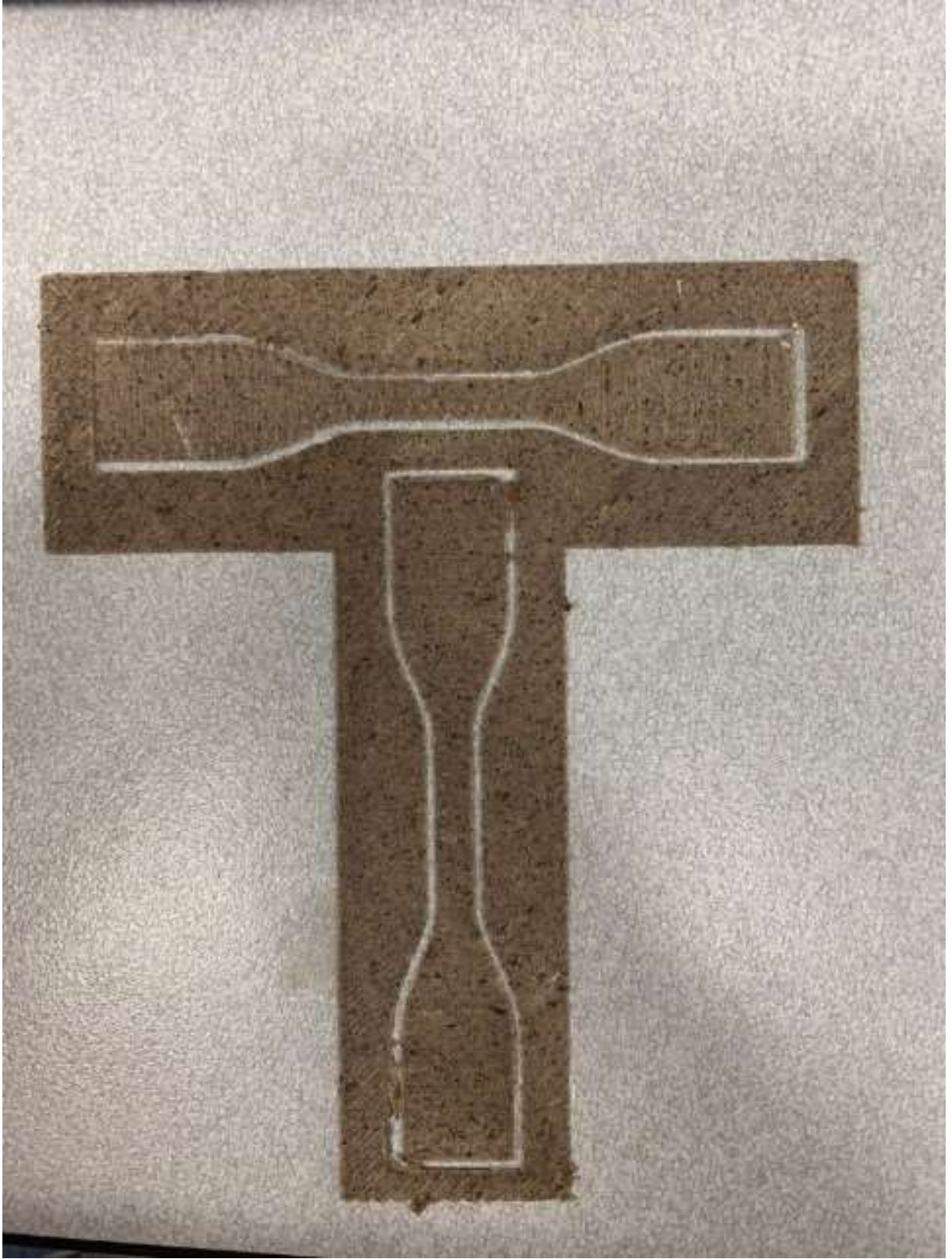**Figure 26**. 3D printed tear test specimen with ABS-SFRC

Figure 27. 3D printed single layer tensile bars with ABS-SFRC

Applications and Outreach

For outreach, the filaments were shipped to an NGO and a community college to get their feedback and explore potential applications.

The NGO (Field Ready) is involved in humanitarian aid supply made-in-the-field. Provided with the Hytrel composite filaments, they successfully printed replacement parts for medical devices (Fig. 4). They commented on the flexibility of the material and application as a substitute for parts made with rubber. They observed that with these filament parts could be printed faster than with common thermoplastic polyurethane filament and parts will maintain sufficient flexibility and strength.

Figure 28. Parts 3D printed by Field Ready with soyhull fibers reinforced HYTREL filament.

Somerset Community College in Kentucky offers degrees in various fields including 3D printing. Spools of Hytrel composite filaments were shared with them. Some of the parts printed by them are shown in Fig. 5. They have also provided valuable feedback by commenting on the shock absorption properties of the material and suggesting potential products that can be explored.

Figure 29. 3D printed parts with Soybean fibers filled HYTREL by somerset community college

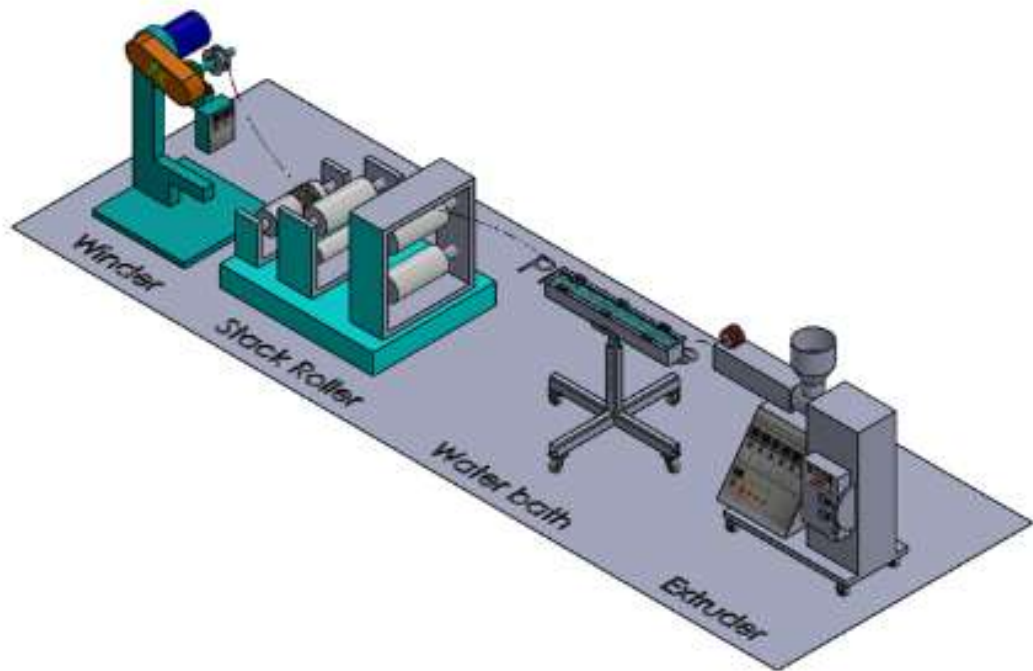# APPENDIX B: 3D MODELS OF FILAMENT EXTRUSION AND 3D PRINTING
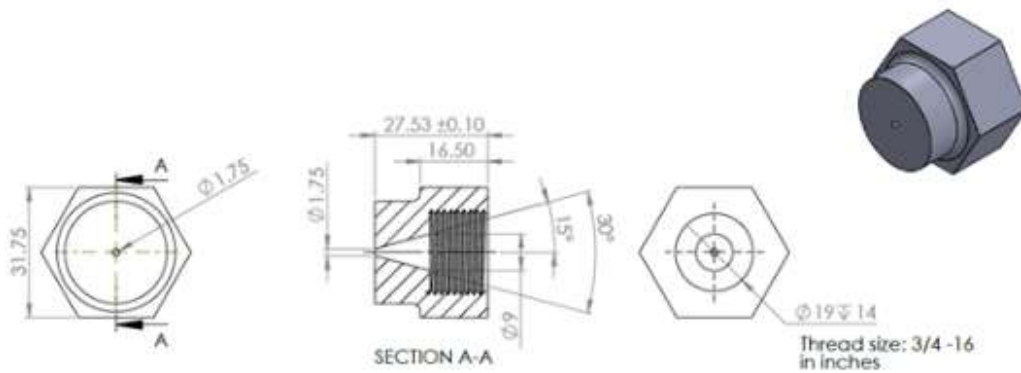
COMPONENTS

Figure 30. Filament extruder setup

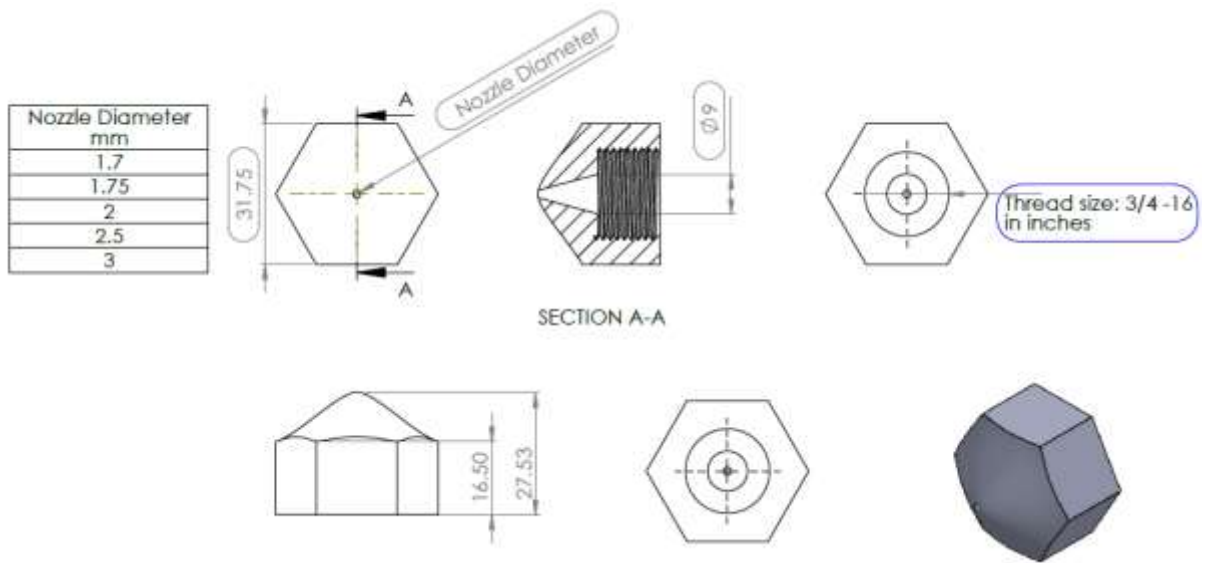**Figure 31**. Custom design nozzle for the pilot extruder

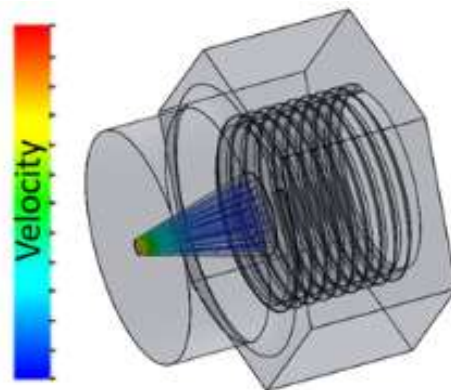**Figure 32**. Variable nozzle sizes design for the pilot extruder

Figure 33. Flow simulations on the nozzle to confirm the effectiveness of the design
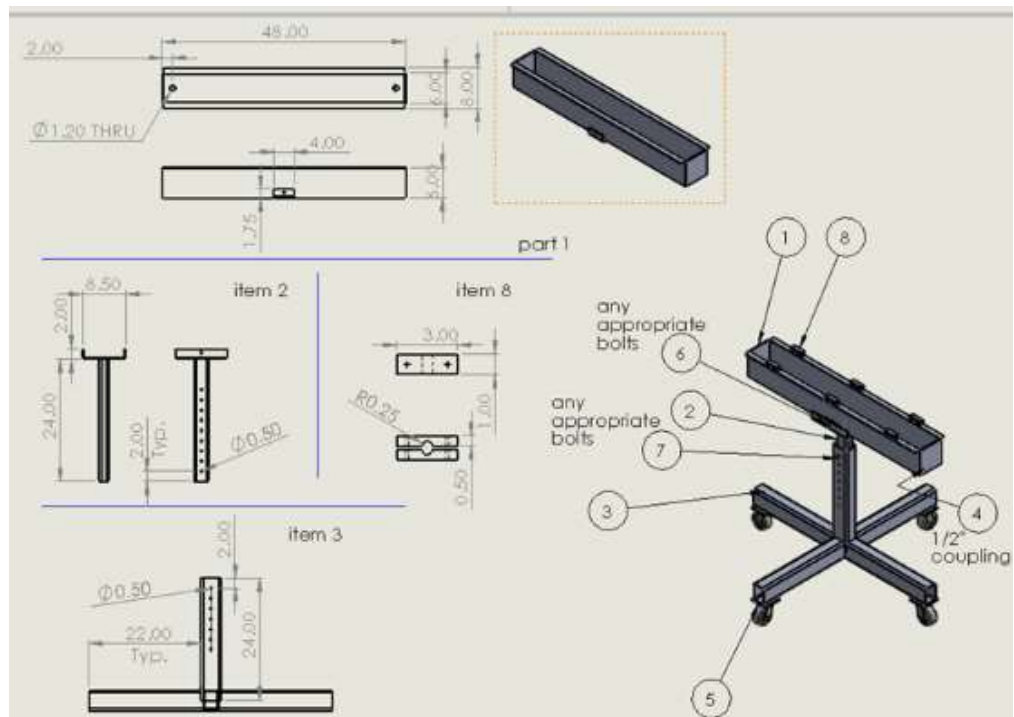
Figure 34. Manufactured nozzle

Figure 35. Custom-designed water bath for the filament coming out of the extruder.

3D printing process conditions

3D printing studies were conducted with all the filaments produced to determine the print processing window. Table below shows the print conditions experimentally determined to be suitable for printing the composite filaments. These processing conditions are needed for commercialization as they will be included in the product datasheets of the spools of 3D printing filaments.

Table 7. Print conditions for the composite filaments.

	Hytrel Composite	ABS Composite	PLA Composite
Nozzle Diameter, mm	0.75	0.75	0.75
Nozzle Temperature, °C	210 - 230	260 - 280	210 - 220
Bed Temperature, °C	50 - 80	80 - 95	55 - 65
Print Speed, mm/s	20 - 100	10 - 40	10 - 40
Extrusion Multiplier	1 - 1.05	0.75 - 1.05	0.75 – 1.05

CURRICULUM VITA

NAME: Saleh Khanjar

ADDRESS: 5505 Symington ct. Louisville KY 40241

DOB: Jeddah, KSA – October 31, 1995

EDUCATION
& TRAINING: A.D., Computer Networking
ASIA E University
2013-2015

B.S., Mechanical Engineering
Gaziantep University
2014-19

M.S., Mechanical Engineering
University of Louisville
2020-21

AWARDS: I-CORP Student Grant Recipient
2020

PROFESSIONAL SOCIETIES:

American Society of Mechanical Engineers
2020-

PUBLICATIONS:

DIGITAL DESIGN AND MANUFACTURING WITH THERMOMECHANICAL

PROCESS SIMULATION FOR FUSED FILAMENT FABRICATION 3D PRINTING.

WORK EXPERIENCE:

Research Assistant
University of Louisville
2020-21

Technology Ambassador
MSC Software
2021

Mechanical Design Engineer
EASI Engineering
2020-21

Design Engineer
MXD Process
2019-2020

Mechanical engineer intern
Bielesko-Biala University
2018

Researcher / Translator
Hacettepe University
2018

Translator
Arche-Nova
2017

Mechanical engineer intern
Kupar Pumpa
2016